Study of Online Driver Distraction Analysis using ECG-Dynamics

by

Shantanu Vijayrao Deshmukh

A thesis submitted in partial fulfillment
of the requirements for the degree of
Master of Science
(Computer and Information Sciences)
in the University of Michigan-Dearborn
2018

Master's Thesis Committee:

Assistant Professor Omid Dehzangi, Chair
Professor Kiumi Akingbehin
Associate Professor Di Ma

To my parents and my grandmother (Late. Suman Deshmukh)

Cultivation of mind should be the ultimate aim of human existence.
- Dr. B. R. Ambedkar

Education is the manifestation of the perfection already in man.
- Swami Vivekananda

Acknowledgements

I would like to thank my supervisor, Prof. Omid Dehzangi, for his kind guidance, encouragement and advice. I consider myself extremely lucky to have a supervisor like him who cared about my work and also let me research with free wings. His constant motivation and timely guidance has helped me to compile this study. I would also like to thank all the members of staff at The University of Michigan – Dearborn who helped me during this study.

.

Table of Contents

List of Tables

List of Figures

Abstract

Majority of the road fatalities occur due to a common cause of human error while driving. Distracted driving is one of the most important contributors to road disaster, because it involves temporary suspension of driver's vigilance while driving. This hypo-vigilance can occur through variety of ways such as talking on cell-phone, texting, conversing with passenger, etc. In order to minimize threats happening across the hypo-vigilance through driver distraction, it becomes highly essential to characterize and identify distraction. During the last decade, many research investigations were conducted on driver state estimation. Particularly, Electroencephalography (EEG), camera-based systems, and behavioral data analysis. Although those systems achieved high empirical performances, there are serious roll block to adopt them practically such as privacy issues, detection latency, or intrusiveness. In this study, we investigate continuous Electrocardiogram (ECG) signals to monitor physiological changes during normal vs. distracted driving in an on-road recording experiment. ECG-based driver state detection is particularly of interest due to its being easy to wear/embed, reliable and minimally intrusive recording technology, and its high signal to noise ratio recording. In this paper, we generated a set of ECG-based measures in order to characterize and identify common pre-defined distracted scenarios. Our aim is to provide an empirical approach for accurate analysis of driver distraction. In this study we introduced distraction by 1) hand-held phone conversation, 2) driver conversation with a passenger next to him, and 3) driver texting on phone while driving. Our effort primarily focuses on the efficient characterization of distraction while driving via localizing R-R interval series based on temporal features as well as spectral features. In addition to this, we further

investigated different short window sizes on the ECG recording stream for real-time predictive ability of the extracted features through state of the art predictive algorithms. Our experimental analysis demonstrated ~92% average predictive accuracy of driver distraction identification in near real-time. In the later part of this study, we also achieved the secondary workload estimation while driving by introducing wavelet as a filter bank approach, this method performed significantly well, yields an open door on spectral analysis in greater depth.

Chapter 1 Introduction

The machine learning system for efficient detection of driver distraction presented in this thesis has two important underlying approaches, 1) Temporal Analysis and the 2) Spectral Analysis. In order to enhance the proposed system predictive capabilities, the features captured with respect to time and frequency domain have to be sufficient enough to derive real-time effective detection of secondary workload while driving. Since the distracted driving is a serious concern, because of its threat to not only the drivers and accompanying passengers but also to the other vehicles moving on the road. Referenced at the research article published in National Highway Traffic Safety Administration (NHTSA) (NHTSA Driver Safety Handbook, 2013) distraction can be characterized into three main groups: 1) Manual distraction taking hands of the steering wheel, 2) Cognitive distraction taking driver's attention off the driving task, and 3) Visual distraction taking eyes off the driving. The observations made during the study in (NHTSA Driver Safety Handbook, 2013) showed that texting while driving is accounted as the combined effect of all three groups of distraction resulting in higher chances of unavoidable accidents. In another investigation it was shown that sending or reading a text message takes eyes off the road for about 5 seconds, which is long enough to cover a football field while driving at 55mph (National Highway Traffic Safety Administration. Facts and Statistics, 2017). Similarly, other types of distractions such as conversing either on a cellphone or with a passenger were shown to pose significant contribution on roadway disasters. NHTSA claims 3,477 number of lives and 391,000 number of people injured in 2015 (Traffic Safety Facts, 2011). After considering the serious hazards of distracted driving it becomes an essential task to localize the

distraction points associated in the training data more effectively and cautiously addressing the real-time approach in seconds of time (called windows in this thesis). In this work, we aim to explore the causality relationship between physiological changes in the ECG signals and distracting scenarios by effectively characterizing changes in the physiological state of the driver. As mentioned earlier our goal is to extract well-established ECG specific temporal as well as spectral measures which enrich the relevant information feature set for efficient prediction as the end goal.

1.1 Current Methods in Estimating Secondary Workload

There has been an extensive research in the field of distraction detection and possible prevention. Wide variety of studies were directed towards, analyzing behavior and subsequent performance contributing driver distraction. In a previous work (O. Nakayama, T. Futami, 1999), the authors made a use of steering entropy in order to calculate an intensity of driver's secondary workload associated with distraction while driving. Observed steering entropy as a promising factor illustrated direct correlation with the amount of effort involved in secondary workload other than driving. However, the steering entropy directly depends individual way of driving being highly subjective measure. Moreover, the resulting detection is latent in terms of the amount of time before a potential accidental threat.

Likewise, there has been much efforts directed towards real time video processing systems to detect distracted driving scenarios. Authors (Wang Rongben, Guo Lie, 2004) detected mouth yawning events using dashboard-mounted closed-circuit camera. The recorded movements tend to be in exact proportions of the amount of fatigue drivers were undergoing while driving. In another related work, authors used two mobile based cameras to monitor and detect driver distraction and fatigue (C. You, 2012). Where the route mapping is achieved using rear-facing

camera of a cellphone while the driver's movements were monitored by the front-facing camera. In another work, the authors investigated state of the art visual systems; available to estimate the secondary workload while driving (A. Fernández, R. Usamentiaga, 2016). However, shown to be effective, camera-based systems have serious privacy issues; which might be a road block to be adopted by the end consumers. Also, the signs of distraction are captured only when they became apparent through video recording (e.g. eye closing); which might be rather late to avoid negative impacts.

Therefore, we believe alternative research expeditions need be encouraged with major focus on the pre-requisites of driver distraction. We envision that there is a causality relation between changes in the physiological state of the drivers and his/her behavior and eventually the driving outcome. Those physiological changes can be captured in forms of bio-signals like as Electroencephalogram (EEG) and Electrocardiogram (ECG). In (Alizadeh Vahid, Omid Dehzangi, 2016), authors suggested using EEG as a way to detect driver distraction. EEG has been proved that is a reliable method as it achieved the accuracy > 90%. However, EEG implementation suffers from intrusiveness, which, in turn, might hinder the applicability of it in real driving scenarios. On the other hand, EEG-based systems due to the high dimensionality of the collected data is very complex and costly for practical and on-line applications.

On the other hand, wearable technology is emerging in various consumer products such as today's smart watches using Photoplethysmographic (PPG) sensors and smart necklaces using Electrocardiogram (ECG) sensors. The ease of deployment is the main advantage of PPG sensors. The tiny PPG sensor can rest at the back panel of a smart watch and measure the real-time blood volume changes in the wrist, even the smart phone camera can record PPG and ultimately measure the heart rate (R. C. Peng, X. L. Zhou, 2015). Recently much research effort

has been put in this area. Author in (András Bánhalmi,1 János Borbás, 2017) measure the Heart Rate (HR) and Heart Rate Variability (HRV) using PPG signals acquired by smart phone camera. Then, they extracted 50 different features from PPG and analyzed their performance with ECG features from the same subjects, found high correlation in both of these feature sets. Similarly, the optical approach of recording PPG is observed in (Z. Cohen and S. Haxha, 2017) where the authors used prototype ring sensor for continuous monitoring of blood pressure, inferred ±5% similarity in the true value of blood pressure using low cost PPG ring device. While PPG is low cost, non-invasive, and easy to record, the main problem with PPG is with the high interference of motion artifacts (MAs) in the recorded PPG data. MAs in PPG acts as pseudo-periodic (Z. Zeng, Z. Pi, 2014) signal that involve with the original PPG thus makes it very difficult to clean, and potentially hampers the quality of recorded data. In order to avoid this problem, many researches have focused on developing MA free PPG using sparse analysis, constrained RLS, joint principal component analysis as seen in articles (Z. Zeng, 2015), (M. S. Islam, 2017), and (A. Galli, G. Frigo, 2017) respectively.

However, there is always a level of uncertainty in the signal quality of PPG which might induce biases in the biomedical inference of physiological changes during distracted driving. ECG on the other hand is a reliable physiological modality to measure driver distraction because of being an easy to wear and record technology, highly reliable with high signal to noise ratio and minimal intrusive implementation. ECG signals are used as the ground truth to estimate the reliability of other technologies such as PPG to estimate critical measures such as HR and HRV such as in (Z. Zeng, Z. Pi, 2014), (D. Jarchi, A. J. Casson, 2016) and (D. Jarchi, A. J. Casson, 2017). Research studies on ECG signals are widespread and continuously growing. Entropy analysis of ECG data has yielded promising results with respect to modeling distraction in a

simulated driving task (L. Yu, X. Sun, K. Zhang, 2011). The authors employed sample entropy (spectral feature) to analyze pre and post distraction behavior of ECG signals. It is observed that the sample entropy associated with post-distraction ECG data has a higher value than pre-distraction ECG. Similarly, authors of the work conducted in (M. Mahachandra, Yassierli, 2012) compare the sensitivity of the extracted features (called indicators of sleepiness) in time and frequency domain analysis of ECG signal to detect sleepiness while driving. More recent investigations such as in (I. Bichindaritz, C. Breen, 2018) used feature selection and machine learning techniques applied on ECG data to monitor stress leading 100% accuracy. Authors in (K. Ito, S. Usuda, 2018) evaluated feelings of excitement using augmented VR technology, placing ECG as a point of reference to indicate feelings. They observed the standard deviation of R-R interval (SD_RR) and R-R interval variability (RRVs) are significant measures to determine the changes in their model of feelings. Similarly, in our previous works in (S. V. Deshmukh and O. Dehzangi, 2017) and (S. Deshmukh and O. Dehzangi, 2017) we observed the spectral side of ECG features with the robust yet effective side of symmetric wavelet as a filter bank approach.

1.2 Data Collection Platform

At University of Michigan-Dearborn, Wearable Sensing and Signal Processing Lab (WSSP Lab), we have developed our custom designed heterogeneous sensor recording platform. The platform is capable of recording different modalities of data streams from various sensors, and conduct synchronization in real-time. Multiple physiological and behavioral channels of data are synchronized and processed over time from such as ECG, EEG, Galvanic Skin Response (GSR), motion (acceleration data), and CAN BUS information. Following figures shows the brief overview of the data acquisition platform.

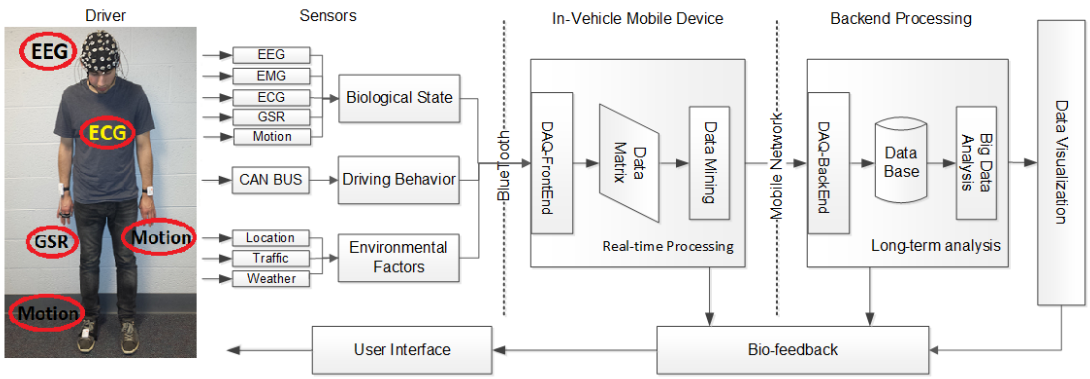

Figure 1:1 Overview of Data Acquisition Platform

1.3 ECG Signal Acquisition

The Electrocardiogram (ECG) is the physiological signal collected from heart. In this study we used Shimmer ECG sensor which records an ECG by simply measuring the electrical potential difference between the purkinje fibers called heart muscles, responsible for systolic and diastolic pressure (called heart beat cycle). The main advantage of using Shimmer sensors is portability in application they are highly portable; sits on the top of chest measures the electrical impulses through leads connected at specific locations using special medical patch. We recorded ECG signals at sampling frequency of 250Hz. While recording 3-lead configuration was fixed for different subjects during the experiments. Each of these leads are then hereafter referred as LE1, LE2, and LE3, respectively. The positions for mounting each of these leads are given in Figure 2. where LE2 is the position where electrodes are closely located to right arm (RA), LE3 is placed near left arm (LA) and left leg position. While LE1 have its position between RA and LA. The following figure shows the shimmer ECG electrode placement and the sensor used in this study.

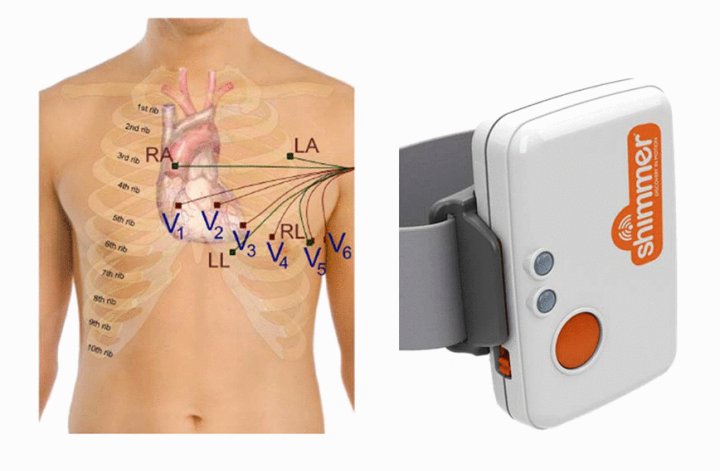

Figure 1:2 Shimmer ECG Electrode Placement Sensor (image source: http://www.shimmersensing.com/images/uploads/docs/ECG_User_Guide_Rev1.12.pdf)

All of the procedures and subsequent actions performed during this experiment were consented based on the University of Michigan Institutional Review Board approval under the submission ID: HUM00102869.

1.4 Distracted Driving Experiment

The one of the major challenges working with ambulatory ECG device is to achieve sufficient precision for characterizing different distraction scenarios and successful identification of distraction. The three-lead configuration used the in this effort is comparatively lower in terms of clinical grade 12 lead configuration, which provides the greater scope of employing advance feature engineering and complex machine learning abilities to minimize the trade-off. Our study did significant job bridging the precision gaps by achieving higher distraction detection accuracy by properly curated experimental procedure. The ECG recording sessions were organized in 12 mins span, divided among each of the driving scenarios including, normal driving on the road (with no distraction elements) for 3 minutes, Phone conversation for the next 3 minutes (phone scenario), question/answering with the passenger (question scenario), and texting while driving (text scenario). The driving route was picked such that traffic, or any other external factors affect

the driving behavior minimally in order for the physiological signals to represent solely the changes occurred due to the impact of the above-mentioned distracting elements. Following figure shows the overview of the distracted driving experiment.

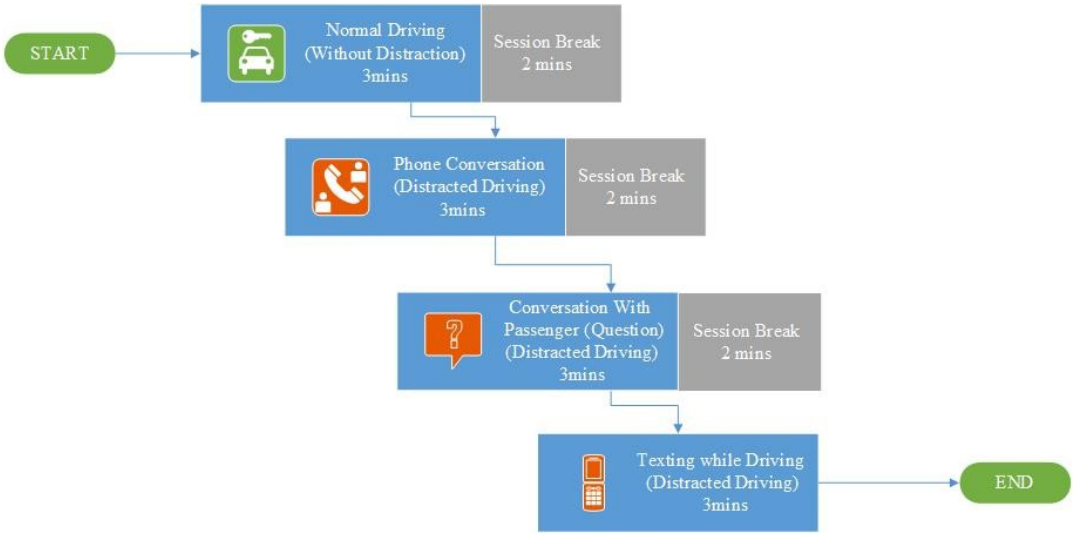

Figure 1:3 Overview of Distracted Driving Experiment

We kept ~2 minutes of normal driving slot in between distraction scenario recordings to minimize the gradual influence of the past driving session on the successive one. Following table, summarizes the whole distracted driving experiment as follows.

Table 1-1Summarized Distracted Driving Experiment

Type	Duration	Significance
Normal	3 min.	when the driver is solely focusing on the task of driving
Phone	3 min.	when the driver engages in a phone conversation while driving
Question	3 min.	when the passenger asks a series of questions in order to engage driver in an active communication while driving
Text	3 min.	when the driver is engaged in between texting while driving

Note: Above distracted driving experiment, projects an upper level abstraction of the approach. Some studies we included extra distraction segment called “text” to emphasize the distracting

capability while in case of modeling spectral analysis using wavelet approach we used three main segments “normal, phone and question”.

1.3 Overview of The Proposed System

As discussed before this effort underlines the complexities included in the real-time driver distraction scoring mechanism. We developed strong (tempo-spectral) feature engineering approach along with Wavelet as a filter bank to score distraction independently. Our overall methodology is shown in the following figure which then can be specified in individual segments.

(draft a figure explaining two bio indicator and wavelet approach on higher level consider following figure as placeholder)

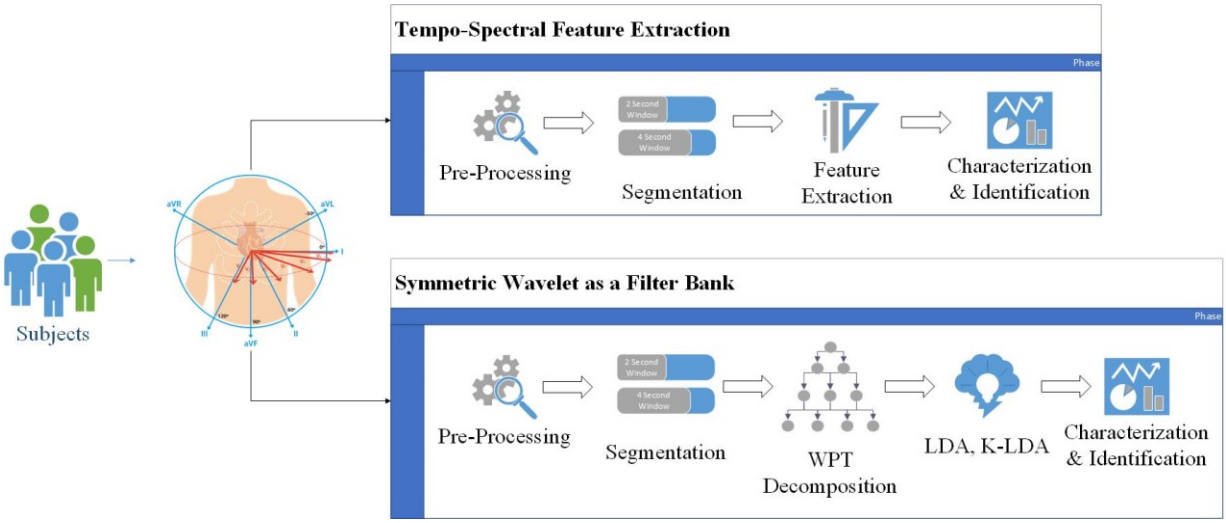

Figure 1:4 Conceptual view of distraction detection system

The above figure forms the basis for our detection approach which then can be explained in more granular sense as follows,

1.3.1 Feature Engineering Approach

In feature engineering approach our intention is to define concurrent relationship between the extracted well established features (called biological indicators) and driver's physiological state. In order to achieve this, we sketched the prosed methodology, covering subsequent steps from pre-processing the input data, segmentation and classifier analysis. We aim to study all possible features which can effectively characterize and identify driver distraction in near real-time. Following figure shows the schematic view of the feature engineering approach.

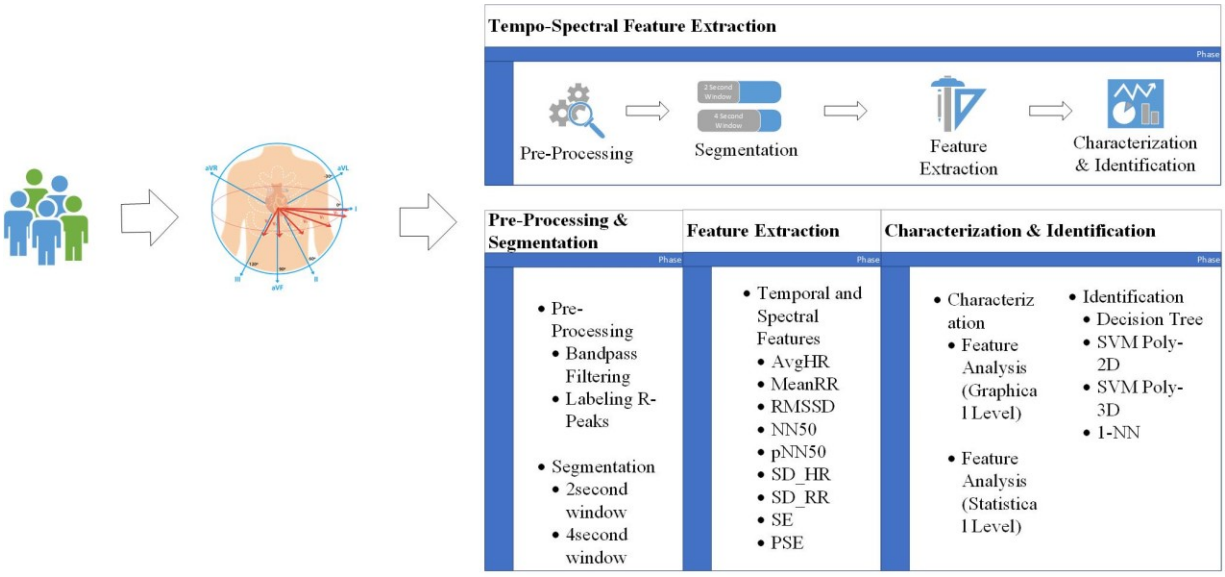

Figure 1:5 Schematic View of Feature Engineering Approach

1.3.2 Wavelet as a Filter-Bank approach

Here in wavelet as a filter bank approach, our goal is to track the fluctuating elements in the ECG signal demonstrating higher deflection in their values due to the distraction scenarios in different frequency levels, ultimately resembling the significant changes in feature space associated with the distracting element. Due to the noisy environment of a vehicle and the nature of physiological signals, Oi, we focus on the spectral analysis of the ECG that can localize noise/artifact activities in certain subBands. We aim to analyze all possible subBands of the ECG

spectrum and treat them as feature values. We then select the subBands with the highest degrees of deflection due to the distracting element, Sti. Then, due to high dimensionality of the generated space and possible chances for curse of dimensionality, we apply linear and non-linear discriminative mapping, φ(Sti), for feature space dimensionality reduction to preserve discriminative capabilities of the target space for predictive analysis. Ultimately, we employ predictive models to the generated discriminative space for model training and evaluation, F(φ(Sti)).

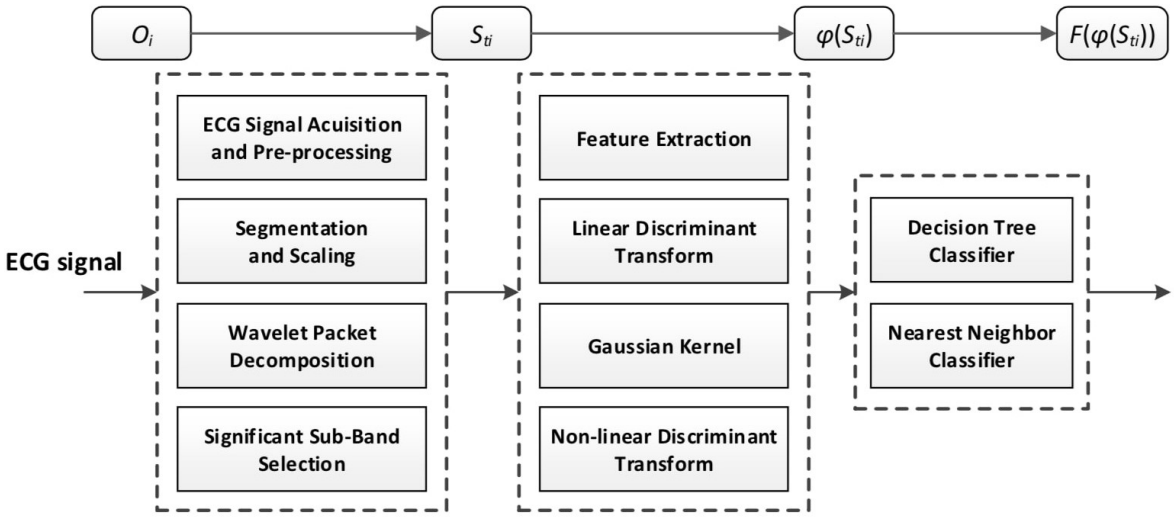

Figure 1:6 Schematic View of Wavelet as a Filter bank approach.

Chapter 2 Temporal and Spectral Feature Engineering

This chapter will cover the temporal and spectral feature extraction technique from raw ECG data starting from cleansing the ECG signal, localizing R peaks, generating features and inferring knowledge from it.

2.1 Segmentation and Pre-Processing

In order to characterize distraction in real time, we implemented segmentation with two different approaches for comparative analysis.

Segmentation approach 1) 2-second window with 75% overlap (25% window increment)

Segmentation approach 2) 4-second window with 75% overlap (25% window increment)

The main intention behind two different window sizes is to locate the signal level noise differences in real-time. In order to address the information flow after segmentation, we treat each block of segmented ECG chain as a separate signal entity throughout feature engineering. Segmentation procedure can be illustrated in depth in following figure 2.1. As mentioned before for comparative analysis 2-second window might induce noise level complexities in detection of distraction as small chunk of 2-second signal might be entirely populated with noise. Another approach of having 4-seond window reduces this noise level complexity with increased computational cost and increase execution time.

As the experiment is conducted in controlled environment with limited movements for driver in-vehicle, having considerably higher signal noise ratio of raw ECG consequently leads to greater

quality of ECG signal with no need to perform advanced sophisticated noise removal techniques in ECG.

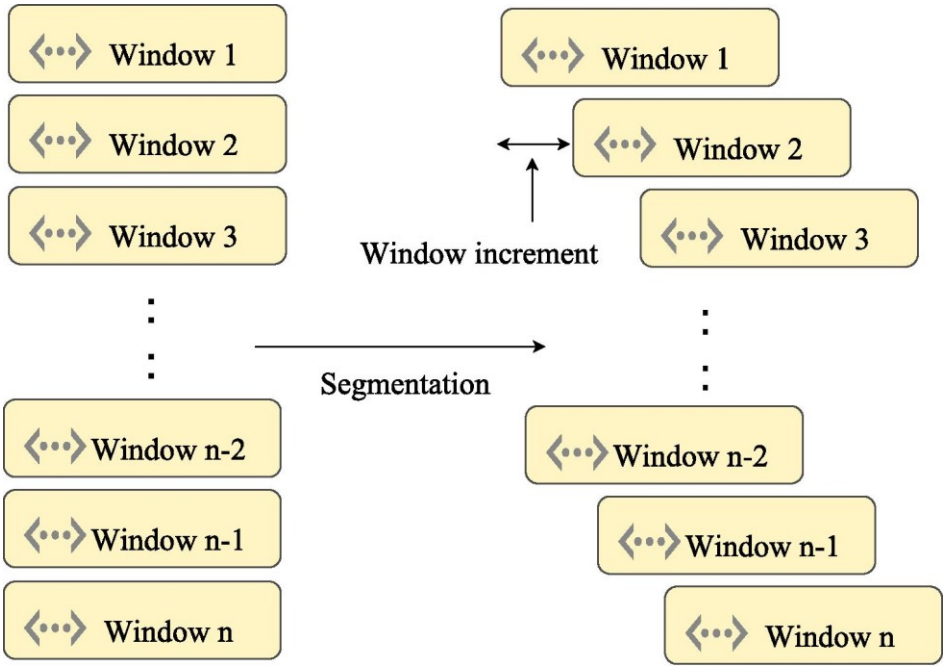

Figure 2:1 Segmentation Approach

At the next stage of pre-processing, raw ECG signal is fed to sharp low pass and high pass filters having cut off frequencies in range of 0.5 Hz to 4Hz. This pre-processing phase helps in removal of high frequency and powerline noises. At the later stages we implemented local maxima detection and labeling of R-peaks. The entire pre-processing module is implemented in MATLAB Software.

2.2 Feature Engineering

We extracted various temporal as well spectral features after segmentation and pre-processing phase. Following table explains the feature name, brief metadata and unit of measurement.

Table 2-1 List of Features with Metadata

Category	**Feature**	**Unit**	**Feature Metadata**	**Equation**
Temporal	AvgHR	bpm	Average heart rate	$\text{avgHR} = \frac{\sum_{w=1}^{N} n_{r_w} \times 60\ seconds}{t_w}$
	MeanRR	ms	Mean of selected R-R series	$\text{meanRR} = \left(\frac{\sum_{r=1}^{n_r} d_{r+1} - d_r}{n_r}\right)$
	NN50	count	Number of consecutive R-R intervals that differ more than 50 milliseconds	$\text{NN50} = \forall(n_r)(nn50++) \leftarrow \sum_{r=1}^{n_r} d_{r+1} - d_r > 50\ milliseconds$
	pNN50	%	Percentage value of count of consecutive R-R intervals that differ more than 50 milliseconds	$\text{pNN50} = \left(\forall(n_r)(nn50++) \leftarrow \sum_{r=1}^{n_r} d_{r+1} - d_r > 50\ milliseconds\right) \times 100$
	SD_HR	1/min	Standard deviation of heart rate	$\text{SD\_HR} = \sqrt{\sum_{rr=1}^{n_r-1} (\alpha_{rr} - avgHR)^2}$
	SD_RR	1/min	Standard deviation of R-R interval series	$\text{SD\_RR} = \sqrt{\sum_{rr=1}^{n_r-1} (d_{rr} - meanRR)^2}$
	RMSSD	ms	Root mean square of differences of the selected R-R interval series	$\text{rmssd} = \sqrt{\left(\frac{(d_{rr})^2}{n_{r-1}}\right)}$

	SE	-	Sample entropy	$SE = -log\left(\frac{(distnace\ vector\ (X_{d(i)})}{(distnace\ vector\ (X_{d+1(j)})}\right) < r \quad where\ (i \neq j)$
Spectral	PSE	-	Power spectral entropy	$PSE = -\sum_{f=-\frac{f_s}{2}}^{+\frac{f_s}{2}} PSD_n(f) \times log_2[PSD_n(f)]$

where,

N = Number of windows

t_w = Sampled time for each window

n_{r_w} = Number of R peaks in each window w

α_{rr} = the heart rate at R-R peak location

$d_{rr} = \sum_{r=1}^{n_r-1} (d_{r+1} - d_r)$

$X_d(i)$ = Distance Vector

$X_d(i) = x_i, x_{i+1}, x_{i+2} \cdots x_{i+m-1}$

PSD = Power Spectral Density

$PSD_n(f) = \frac{PSD(f)}{\sum_{f=-\frac{f_s}{2}}^{+\frac{f_s}{2}} PSD(f)}$

2.2.1 Time Domain Analysis

R-R interval series forms the base of feature extraction in time domain. The R-peak detection process is based on derivative based peak detection algorithm. In which we first calculate the first order and second order derivatives $d_1(x)$ and $d_2(x)$ using (Kher, Rahul, 2010) and (Artega, Falconi, 2015) approaches,

$$d_1(x) = |p(i+1) - p(i-1)| \tag{2.2}$$

$$d_2(x) = |p(i+2) - 2p(i) + p(i-2)| \tag{2.3}$$

After calculation of $d_1(x)$ and $d_2(x)$ we inverse the second order derivative $d_2(x)$, which makes the Inverted Second Derivative (ISD) record. After which we to retain the data structure called SA by sorting out the ISD series in descending order as performed in (Artega, Falconi, 2015) approach. Using this technique, we detect consecutive R-peaks, in which two successive R peaks are considered to be the part of on cycle. Following figure illustrates the R peak detection using ISD method.

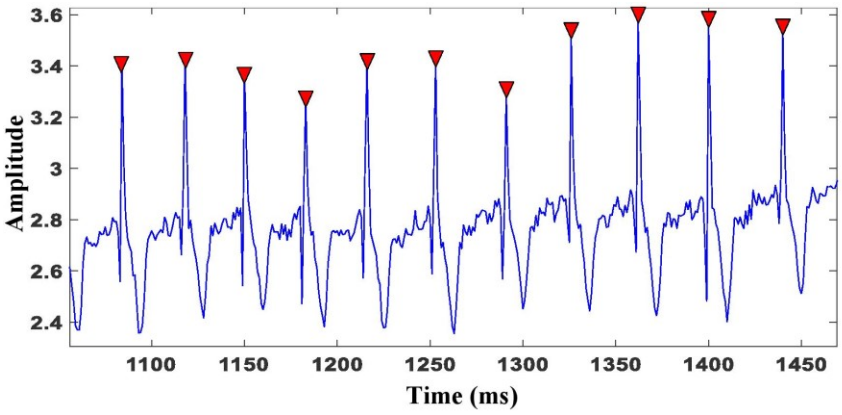

Figure 2:2 R-Peak Detection using ISD Method

As discussed before R-peak detection is an integral part of this study. Most features extracted from time domain analysis are driven by R-peaks. Some useful notations for each of the

following computations, we express the R peaks as r and successive distance between R peaks as d.

2.2.2 Frequency Domain Analysis

While understanding the spectral part of ECG analysis, our focus was mainly on energy distribution analysis. Entropy can be thought of degree or extent of dilution (distraction) to the driving process. We extracted strong Power Spectral Entropy as the measure of an uncertainty in the energy distribution of time series in each frequency. PSE can be thought of a direct relationship between uniformity in energy distribution which means the higher value of PSE the higher would be the energy distribution.

2.3 Identification of Driver Distraction

Once after computation of all features, we performed effective classification using 10-fold cross validation approach on all 4 different classification algorithms used. One Advantage of using 10-CV approach is the optimum use of every part of training set. In 10-CV every part is optimally used in detection phase, by keeping 1 part as test and remaining 9 parts as training in every iteration of 10-CV with 0 overlap.

Classification Algorithms Used:

Decision Tree

Quadratic Support Vector Machine

Cubic Support Vector Machine

Nearest Neighbor

Short summary of each of the predictive algorithm is given below,

2.3.1 Decision Tree (DT)

Decision tree is the widely used predictive algorithm in machine learning (Y. M. Freud & L. Mason,1999). DT represents a tree structured hierarchy in which each non-leaf node is test attribute, which branches out representing output of the test, with each terminal node having class label. Depending on a metrics applied e.g. number of splits etc. there are many DT representations available for construction.

2.3.2 Support Vector Machine (SVM)

Support Vector Machine is a discriminative classifier which aims to optimize the generalization parameter of the trained model based on concept of margin maximization (C. Cortes & V. Vapnik, 1995). An optimal hyperplane is said to be good if when it doesn't pass through majority of points leaving behind larger margin between desired hyperplane and training dataset. We used to type of SVM in our predictive modeling called quadratic SVM (SVM-Poly2D) and cubic SVM (SVM-Poly3D).

2.3.3 K- Nearest Neighbor (K-NN)

K-nearest neighbor (K-NN) is the best example of non-parametric approach in pattern recognition (J. M. Keller & M. R. Gray, 1985). It makes an efficient use of closest neighbor label in feature space to perform classification. It assigns a data point to particular class based on majority of votes among the nearest training points.

We used 1-NN in our predictive modeling.

Chapter 3 Wavelet as a FilterBank

This chapter will cover an effective frequency subBand analysis using Wavelet Packet Transform (WPT) to localize the impact of distracting elements. Due to high dimensionality of the WPT generated space, this chapter will introduce an applied Linear Discriminant Analysis (LDA) approach for feature space dimensionality reduction; preserving discriminative capability of the predictive model. In order to further enhance the prediction ability of the system, we used kernel transformation in order to take into account non-linear interactions of the input feature space. Based on our results, WPT transform in combination with Linear Discriminant dimensionality reduction demonstrated high potentials to detect normal vs. distracted driving scenarios. Using kernel transformation further increased feature space discrimination compared to the baseline features and let to an increase from 44.10% to 88.45% average prediction accuracy over all subjects. Thereby proves the FilterBank property of wavelet.

3.1 Wavelet Packet Transform

Biomedical signals have a brief high-frequency noise component associated with it (R. N. Khushaba & S. Kodagoa, 2011). Wavelets are one of the most popular multi-resolution spectral visualization techniques that can be applied to such signals owing to the resolution. The wavelet packet transforms (WPT) was introduced by clubbing together multi-resolution approximations and wavelets (R. R. Coifman & Y. Meyer, 1992). WPT can be thought of as tree subspaces, with $\Omega_{0,0}$, being the first sub-space i.e. the root node of the tree. In general, each single node in the Wavelet tree can be represented as $\Omega_{m,n}$, where m denotes the current level of decomposition

and n denotes the subBand index within the current level of decomposition. Every level is decomposed into two orthogonal subspaces: approximation subspace $\Omega_{m,n} \rightarrow \Omega_{m+1,2n}$, and detail subspace $\Omega_{m,n} \rightarrow \Omega_{m+1,2n+1}$, (K. Englehart, 1998). This is achieved by dividing an orthogonal basis $\{\varphi_m(t-2^m n)\}_{n\in q}$ of $\Omega_{m,n}$ into two orthogonal bases $\{\varphi_{m+1}(t-2^{m+1} n)\}_{n\in q}$ of $\Omega_{m+1,2n}$ and $\{\psi_{m+1}(t-2^{m+1} n)\}_{n\in q}$ of $\Omega_{m+1,2n+1}$ (S. Mallat, 2009). Where $\varphi_{m,n}(t)$ and $\psi_{m,n}(t)$ are scaling and wavelet functions which are defined in the following diagram, as mentioned in (S. Mallat, 2009).

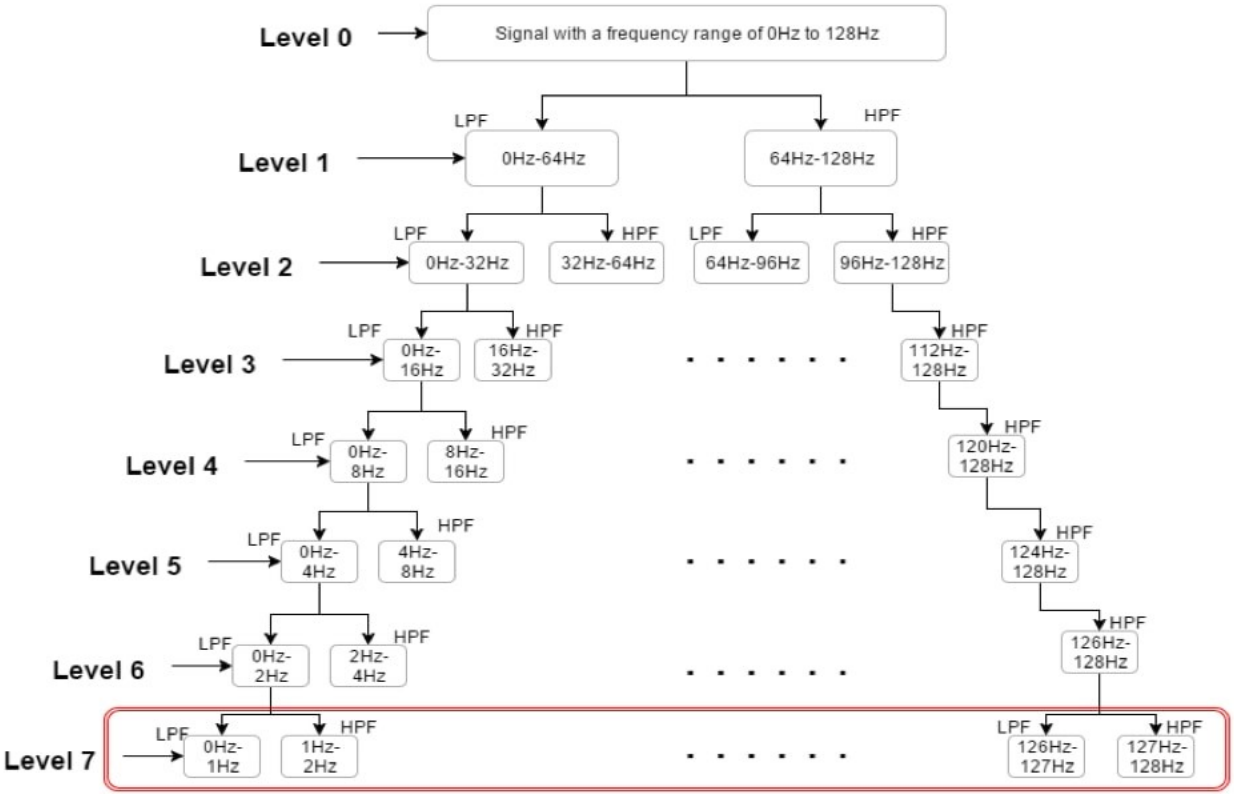

Figure 3:1 WPT Multiresolution Decomposition Tree

$$\varphi_{m,n}(t) = \frac{1}{\sqrt{|2^m|}}\varphi\left(\frac{t-2^m n}{2^m}\right) \tag{3.1}$$

$$\psi_{m,n}(t) = \frac{1}{\sqrt{|2^m|}} \varphi\left(\frac{t - 2^m n}{2^m}\right) \tag{3.2}$$

where 2^m is the compression regularizing parameter also known as the scaling parameter and $2^m n$is the translational parameter which has the time location of the wavelet. Fig. 3.2 illustrates WPT multiresolution decomposition transformation tree.

3.2 Feature Extraction

In the feature extraction phase, we used the multi-signal wavelet packet decomposition method (R. R. Coifman & Y. Meyer, 1992) (R. N. Khushaba & A. Al-Jumaily, 2007) to generate wavelet packet decomposition expressing different frequency subBands. The input from the previous step is fed to this function, and at the output, we get decomposed waveform by seven levels of decomposition based on wavelet family 'db4'. Seven levels of WPT decomposition produces 255 Wavelet coefficients. Each Wavelet coefficient has frequency subBand associated with it. The Wavelet Packet Coefficients spans the frequency range of 0 to 128 Hz. Out of every frequency subBand, we extracted three features named power, mean, and standard deviation.

3.3 WPT SubBand Selection

For the comparative analysis of different features corresponding to the specified frequency subBand, we have conducted the t-test and monitored p-Value as an indicator explaining the statistical difference between two feature values. p-Value captures the significant statistical difference between the feature values of two sample populations (before and after driver distraction).

We generated a measure p = log(1/p-Value) such that the higher the p-Value, the better the subBand. We optimized a threshold of t over log(1/p-Value) of all subBands based on statistical

significance between normal vs. distracted situations. If the p corresponding to a subBand is greater than t, then the subBand is selected.

3.4 Linear Discriminant Analysis (LDA)

We introduced the LDA analysis, to make our model robust to the curse of dimensionality, without affecting overall prediction accuracy. The LDA analysis (Vasilescu M. &Alex O., 2002) is based on emphasizing those vectors that best discriminates among the classes (instead of discriminating those, who best describes the data). LDA basically creates the linear combination of those vectors which delivers largest mean difference between the target class (Liu & Chengjun, 2001). LDA solves the optimal discrimination projection matrix given by W_{opt}.

$$W_{opt} = arg_W max \frac{|W^T S_b W|}{|W^T S_W W|} \tag{3.3}$$

Where S_b and S_W are the scatter matrices given as follows,

$$S_b = \sum_{a=1}^{b} n_a(\mu_a - \mu)(\mu_a - \mu)^T \tag{3.4}$$

or

$$S_W = \sum_{a} (x_a - \mu_{k_a})(x_a - \mu_{k_a})^T \tag{3.5}$$

Where S_b is between class scatter matrix and S_W is within class scatter matrix. Then the total scatter matrix can be formulated by taking sum of S_b and S_W as $S_t = S_b + S_W$. μ_a is the mean feature vector of class a, n_a is the number of samples in class a, and b is the total number of samples in the dataset. x_a is a feature vector of a sample, and μ_{k_a} is a vector of a class a that has x_a.

3.5 Kernel-LDA

As the non-linear extension of LDA, Kernel LDA (Scholkopf & Bernhard, 1998) performs LDA in feature space, φ(Ye & Fei, 2009) using the mapping,

$$\varphi: \gamma \rightarrow \zeta \mid a \rightarrow \varphi(a) \tag{3.6}$$

Where γ is a low dimensional space that represent the data with linearly non-separable class distribution. By using the above-mentioned non-linear mapping, φ, γ transforms to ζ (i.e. $\gamma \rightarrow \zeta$) which is a high dimensional space in which different classes of data are linearly separable. Now I can rewrite the objective function using φ in 3.6 as:

$$W_{opt} = arg_W max \frac{|W^T S_b^{\varphi} W|}{|W^T S_W^{\varphi} W|} \tag{3.7}$$

Where,

$$S_b^{\varphi} = \sum_{a=1}^{b} n_a (\mu_a^{\varphi} - \mu^{\varphi})(\mu_a^{\varphi} - \mu^{\varphi})^T \tag{3.8}$$

or

$$S_W^{\varphi} = \sum_{a} (\varphi(x_a) - \mu_{k_a}^{\varphi})(\varphi(x_a) - \mu_{k_a}^{\varphi})^T \tag{3.9}$$

Where feature vector of samples in a new dimension is $\varphi(x_a)$, μ^{φ} is the average of all the data, and $\mu_{k_a}^{\varphi}$ is a mean of class a in the new space. One of the popular kernel function is Gaussian Kernel which can be given as,

$$\mathrm{K(a, b)} = \exp(-\frac{\|a - b\|^2}{\delta}) \tag{3.7}$$

3.6 Distraction Identification Task

In this section we used four different cases for comparative analysis of prediction accuracy. Explained as follows:

1. **Baseline:** Consist of last level wavelet coefficients of wavelet packet transform tree. Total number of 128 wavelet subBands constitutes 128 features at the last level.
2. **subBandSelect:** Consist of selected subBands based on their individual contribution to the identification task of distraction. In our effort we have subBand select data of ~20 selected subBands.
3. **subBandSelect + LDA:** This consist of combination of subBandSelect approach along with LDA discriminative dimensionality reduction technique.
4. **subBandSelect + Kernel + LDA:** In this case there is an introduction of kernel transformation after subBandSelect approach combined with LDA analysis at the end. Here we used Gaussian Kernel with variance=1.0

All of the above 4 feature sets are accessed by employing them into classification learner using decision tree and 1-nearest neighbor (1-NN) (Safavian & S. Rasoul,1991) (Larose & Daniel, 2005). All of the classification tasks are performed with 10-fold cross validation (10-CV) (John Lu & Z. Q., 2010). The main reason behind employing 1-NN in the feature space is to model the complexities involved in different feature spaces by using 1-NNs instance-based method.

Chapter 4 Results and Discussion

With an envision of causality relationship between physiological changes and the driving outcome. Our proposed distraction identification system has shown significant results supporting this fact, including feature engineering and wavelet approach.

4.1 Results (Feature Engineering Approach)

We investigated different features on graphical as well statistical scale, observed remarkable in depth understanding of extracted features called biomarkers.

4.1.1 Individual Feature Analysis (Graphical Analysis)

We inferred that there is a direct correlation between heart rhythm to driver's state of mind. Our experimental analysis showed higher value of average heart rate (AvgHR) while the driver is undergoing distraction. Following figure 4.1 shows AvgHR and AvgHRV over all subjects. Similar to the increasing AvgHR values we observed an inverse trend in AvgHRV values throughout all subjects. Figure 4.2 shows this trend markers from subject 1 with test time of ~20 minutes. Observing the trend line plot at figure 4.2 we can say that the trend of inverse relationship over AvgHR and AvgHRV is consistent. From this consistent trend we can infer that constant increase in heart rate can be observed with subsequent decrease in heart rate variability when the driver is in excessive state of mental workload. We can relate this mental workload to the secondary activates called distraction while driving, with an empirical proof gathered from this study. Similar to AvgHR and AvgHRV we extracted/engineered 8 different features from

temporal and spectral space, which can be visualized in the following figures from figure 4.3 to 4.11. The results from these 8 biomarkers presented more insights in the pursuit of exploring physiological changes with respect to time; in normal, phone (phone conversation while driving), question (conversation with passenger) and texting (texting on phone while driving scenarios).

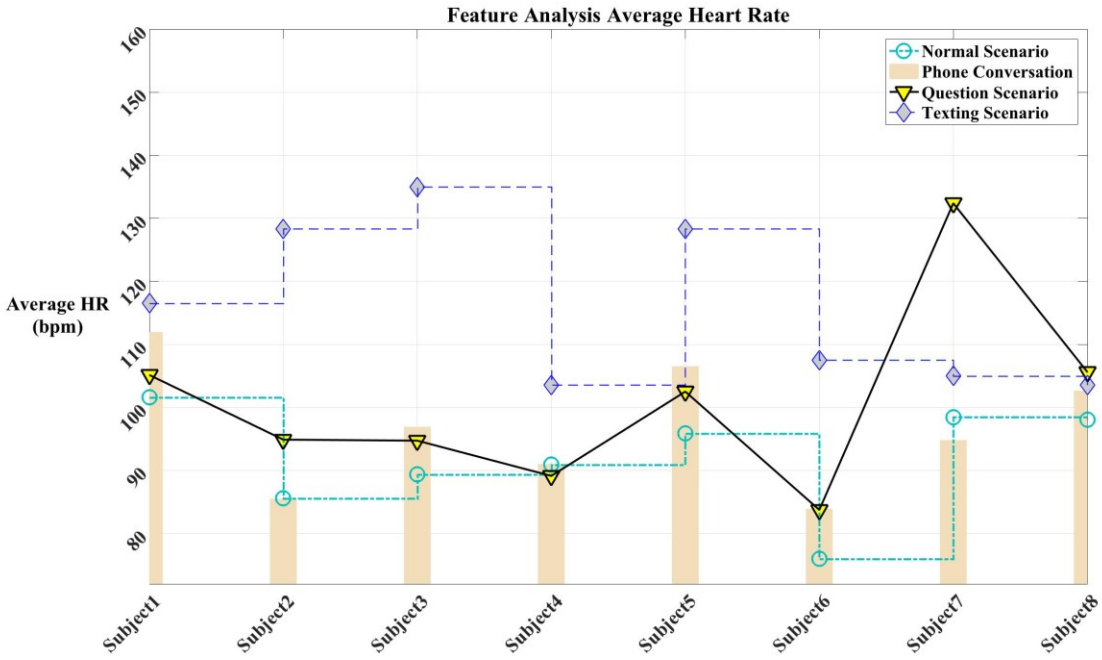

Figure 4:1 AvgHR over all Subjects

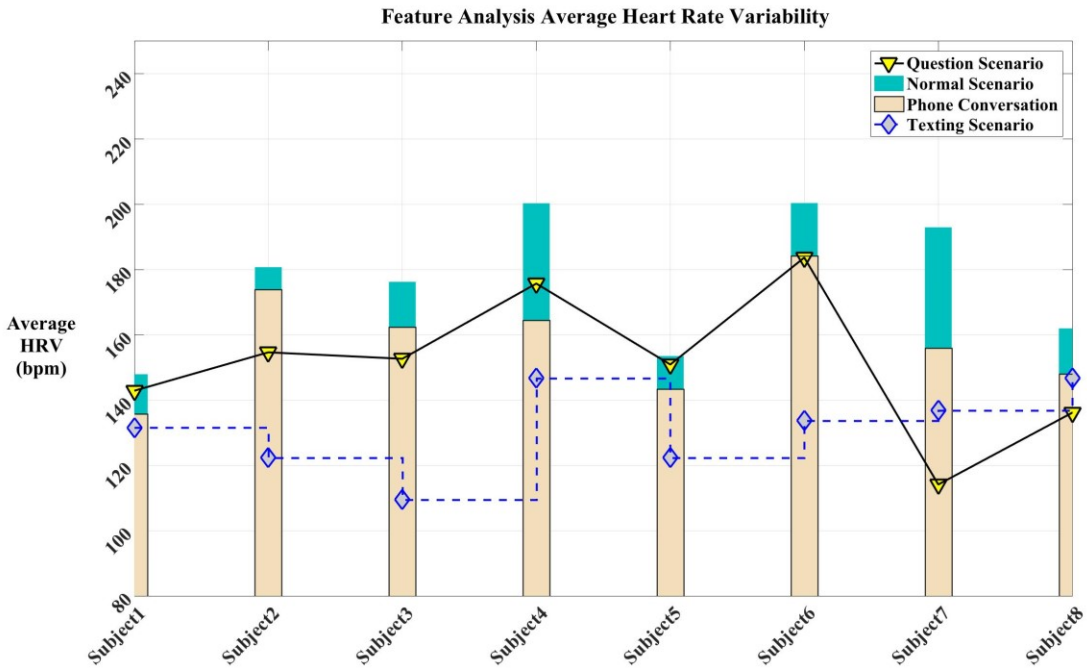

Figure 4:2 AvgHRV over all Subjects

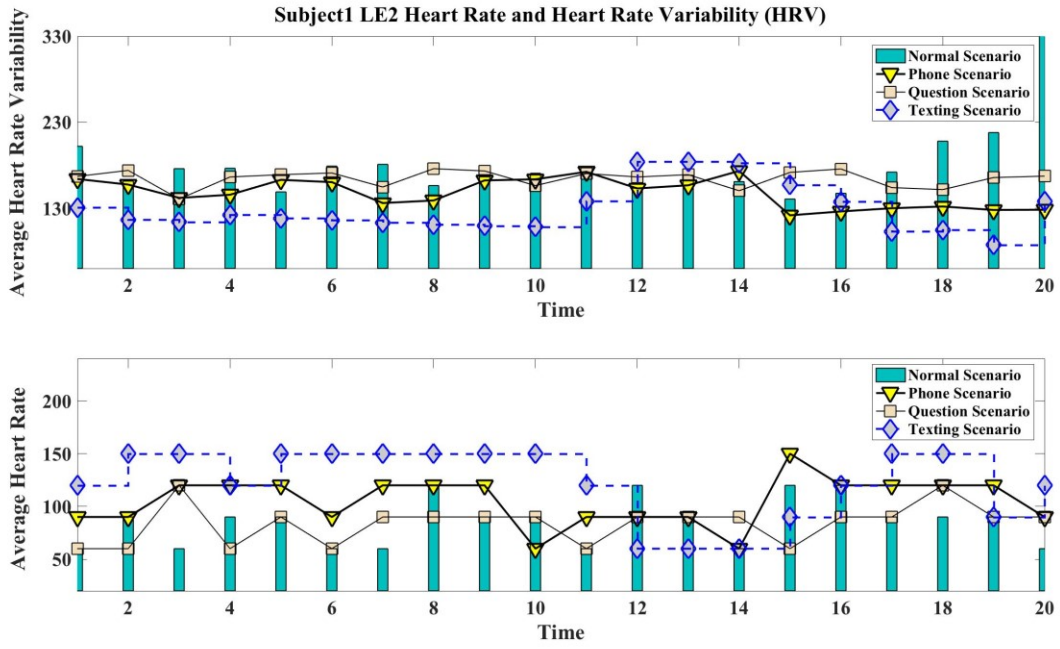

Figure 4:3 AvgHR and AvgHRV Continuous Trend Marking Plot of 20 minutes

Following table represents the list of bio-markers and their associated figure names.

Table 4-1 Figure Mapping with Explained Feature Plot

Figure	Feature Plot
4.4	MeanRR
4.5	NN50
4.6	pNN50
4.7	SD_HR
4.8	SD_RR
4.9	RMSSD
4.10	SE
4.11	PSE

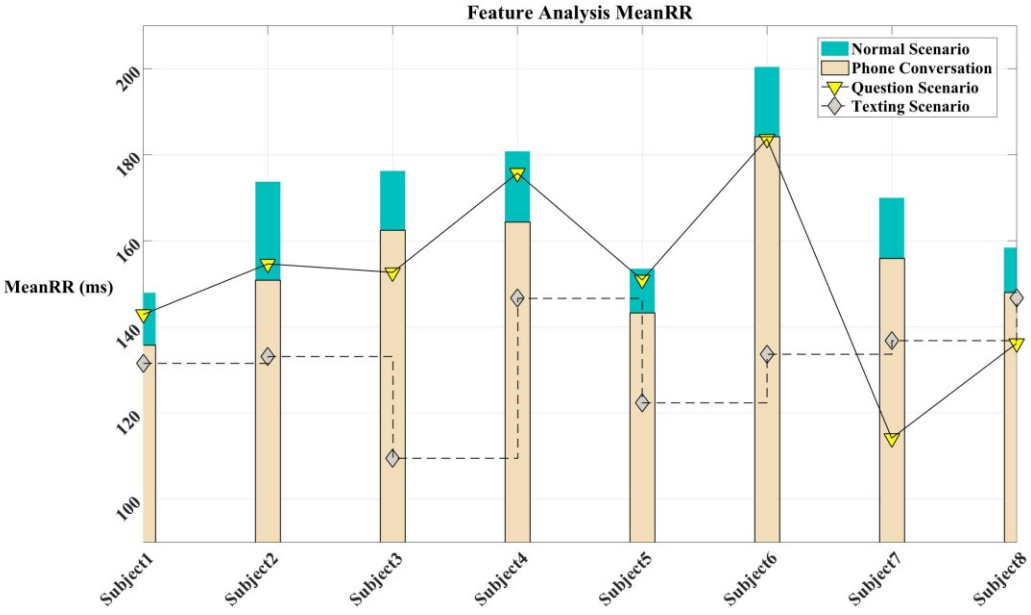

Figure 4:4 Feature Analysis Plot - MeanRR

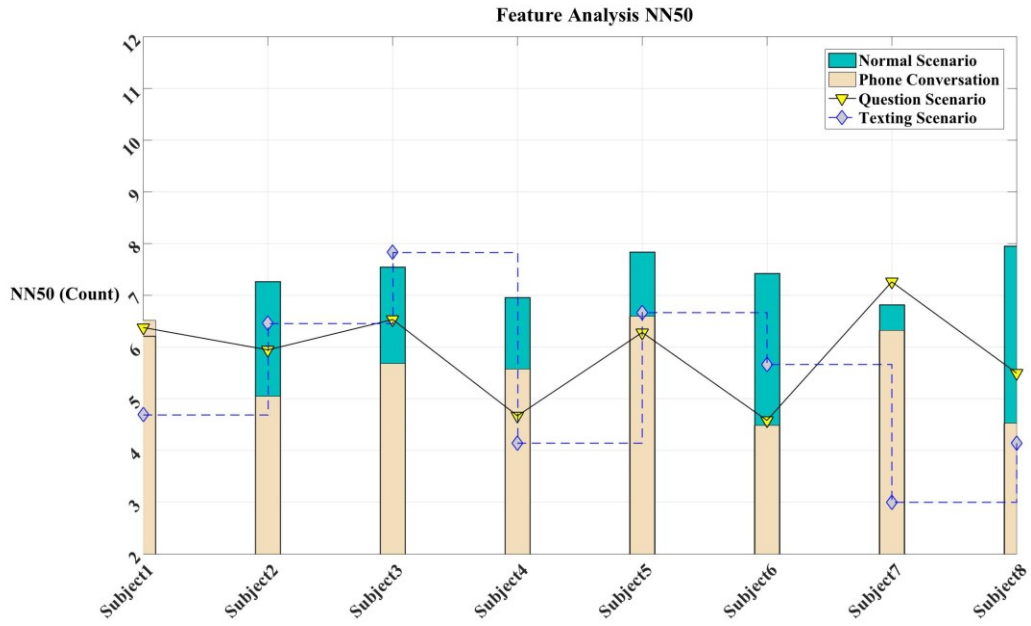

Figure 4:5 Feature Analysis Plot - NN50

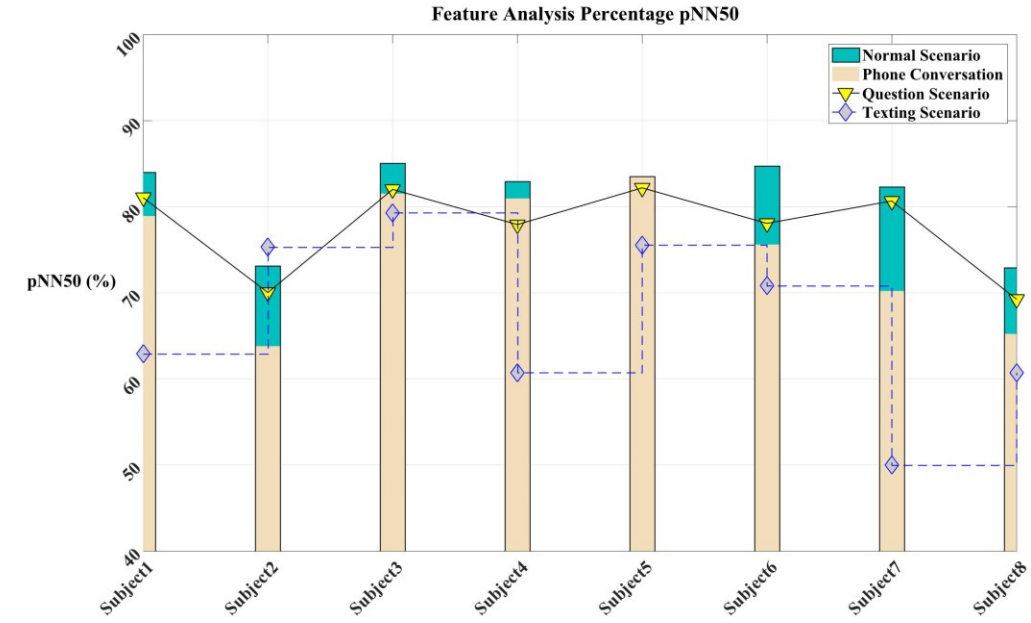

Figure 4:6 Feature Analysis Plot – pNN50

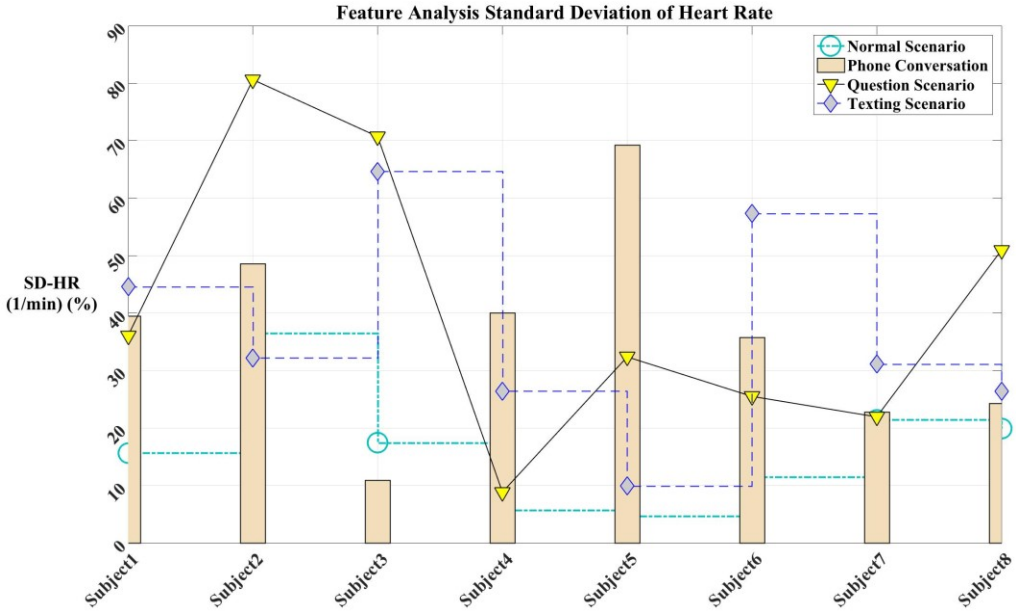

Figure 4:7 Feature Analysis Plot – SD_HR

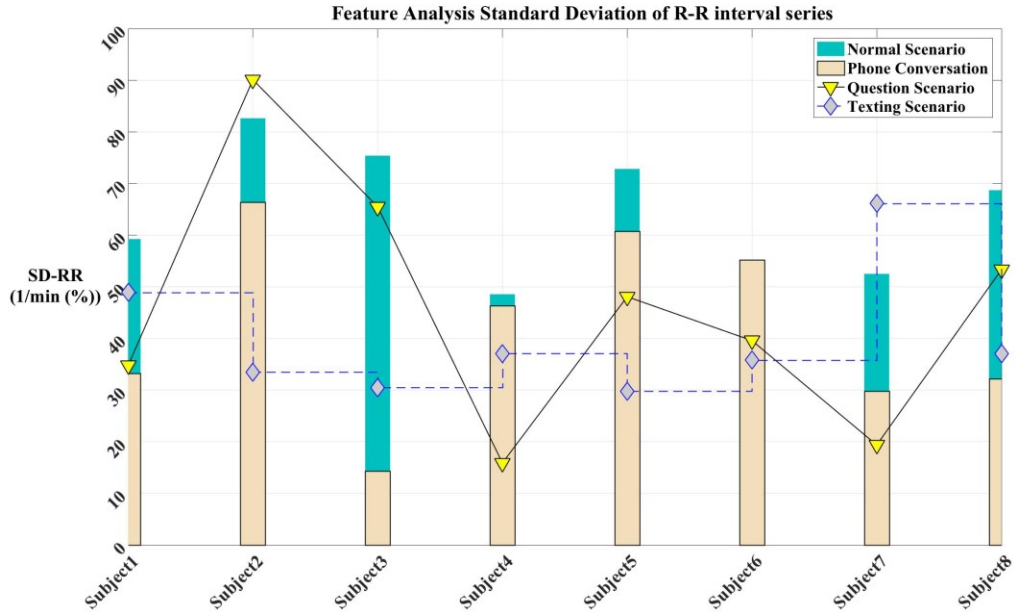

Figure 4:8 Feature Analysis Plot – SD_RR

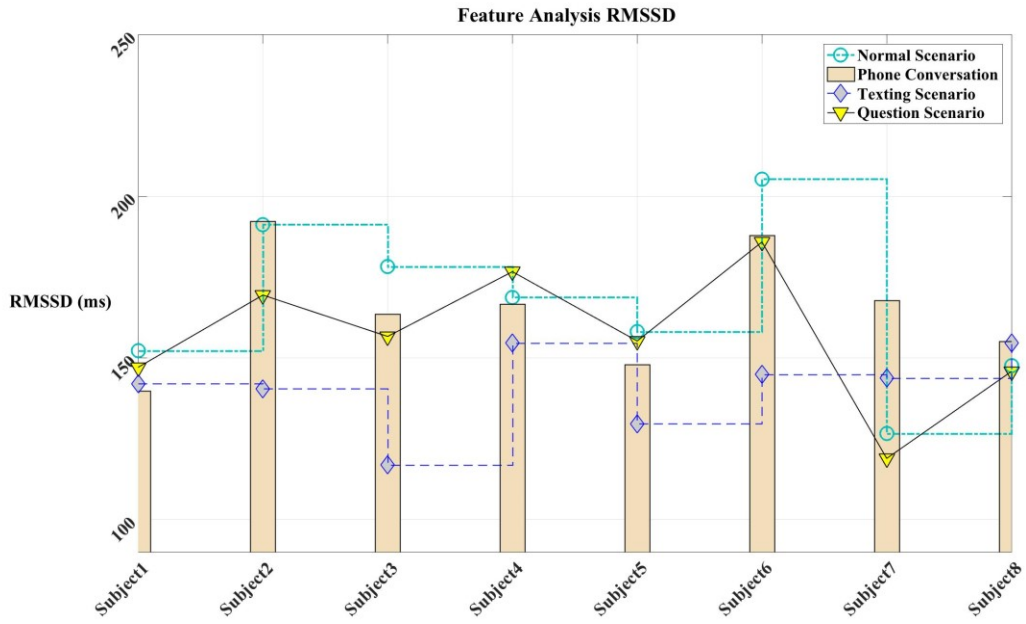

Figure 4:9 Feature Analysis Plot - RMSSD

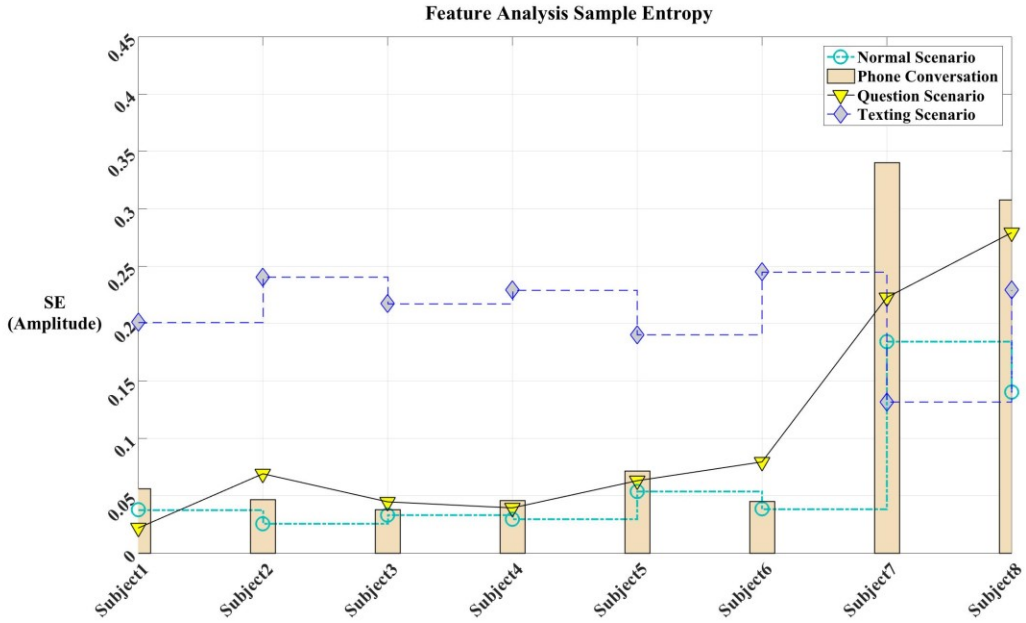

Figure 4:10 Feature Analysis Plot - SE

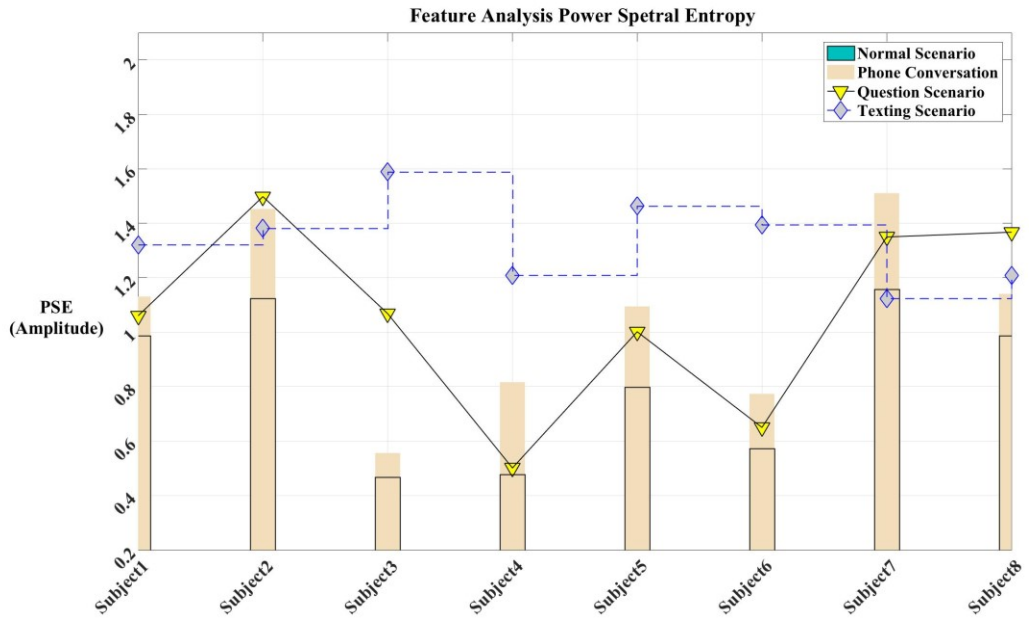

Figure 4:11 Feature Analysis Plot - PSEObserving the first bio-indicator meanRR in figure 4.3 we can state that the distance delta between two successive R-R peaks, gets higher value in normal driving as compared to the distracted driving with lower value. Which emphasize the foundation of timing gap (referred distance between two R-R peaks) gets bigger with subsequent decrease in heart rate. Since heart rate is inversely proportional to the distance between R-peaks. Hence increased value meanRR in normal scenario denotes lower heart rate and decreased value of meanRR in distracted scenarios indicate higher value of heart rate as discussed in equation 4.4. Similar to this we can observe decreasing trend in the values of standard deviation of R-R interval series, provides justification to the aforementioned fact that mental workload involved in performing secondary tasks lower the distance between two R-R peaks, enabling higher values of heart rate. Addressing the biological aspect this reduction in heart beats is caused because of the blood regulation in lungs achieved by human heart. Pacemaker in human heart is responsible for maintain blood pressure in body. The articulo-ventricular contraction and relaxation is driven by this pacemaker. While in distracted state of mind driver needs constant supply of more

oxygenated blood towards brain to fulfill the demand of concentration in multitasking (i.e. working on driving and secondary tasks). This increase in demand of oxygen increases the blood flow which tend the pacemaker to send more impulses to heart to contract and relax quicker which ultimately increases the heart rate. All of our extracted bio-markers shows the concrete relevancy to the above facts.

Similar to AvgHR and meanRR similar trend lines have been observed in case of RMSSD feature. Since being the derived part of R-R interval series the, the pacemaker effect has been seen across all RMSSD values. This observation makes strong agreement with proposed article in (A. L. Hansen, B.H. Johnsen, 2003) in which the subjects with higher RMSSD values showed better performance than lower RMSSD values in figure 4.9. This shows concrete relevancy with the amount of workload driver is undergoing through. When the amount of workload is lower (as in case of driving scenario higher RMSSD is observed, while in case of distracted scenarios lower value of RMSSD is seen. SD_RR being another statistical feature derived from the family of R-R derivation series shows similar trends in values, stating lower values of SD_RR in distraction scenarios. Likewise, we investigated NN50 and pNN50 features, which represents the increasing count when timing gap between two consecutive R-R interval series goes more than 50 milliseconds. For example, in figure 4.5 and 4.6 we have greater counts of NN50 and higher percentage values for pNN50 in normal scenarios, which indicates the time separation between consecutive R-R peaks. This fact goes back to our aforementioned statement that when the timing gap between two consecutive R-R peaks get bigger significant reduction in heart rate is observed; as heart rate is the function of count of R peaks in an underlying beat cycle. These observations from NN50 and pNN50 also shows an important insight lying behind the complexities of distraction as we can see the values of NN50 gets lowered when distraction

element gets higher. This circles back to the evaluate the amount of distracting component in each secondary task, from which we can infer that texting while driving being the lest count of NN50 leads to devastating effect of distraction while onboard as discussed in (NHTSA Facts and Statistics, 2017).

Covering more statistical ground, when driver is exposed to distraction scenarios another bio-indicator named SD_HR shows higher values in distraction. Particularly in case of texting while driving as shown in figure 4.7, this proves that maximum level of cognitive load is engaged in texting while driving. In addition to the R-R family derivation features, we evaluated another set of complexity measures called sample entropy (SE) and power spectral entropy (PSE). Both SE and PSE exhibited significant impact quantizing real-time driver distraction by projecting higher values in space while driver is in state of distraction. This observation leads to measure the level of complexity involved in multi-tasking while driving. Figure 4.10 and 4.11 shows these observations. Comparatively there is no specific ups and downs has been in seen in case of normal vs. phone scenarios or in case normal vs. question scenario, the observation seems to sought subjection in these cases. While in case of texting an increase in values has been observed throughout the plot, shows matter of significant concern.

4.1.2 Individual Feature Analysis (Statistical Analysis)

After successful implementation of the graphical analysis we want to give statistical validation touch to the predictive model. For which we have performed score based ranking mechanism. Table 4.3 and Table 4.4 shows the output of our cumulative approach for ranking features. The given figure shows three different cases of comparison named normal vs phone, normal vs. question and normal vs. text. The scores achieved by the corresponding feature can be tracked with the help of given Table 4.3 and 4.4 where, green color represents observed counts achieved

by the feature. Calculated scores are determined as a function of summation of possibilities as a Boolean vector. Whose individual value tends to 1 when the p-value particular to the feature in particular distraction scenario goes less than 0.1 over all subjects.

Observing the pi plot in Table 4.4 we can say that SE showed highest level of statistical significance over all subjects. Similarly, other features such as AvgHR, NN50, pNN50, SD_HR, RMSSD showed consistent performance throughout this statistical validation.

Similarly, in order to further access the credibility on statistical grounds, we averaged p-values corresponding to each subject, figure 4.13 shows the p-value comparative analysis over all features. In which the Y-axis has all the p-value magnitudes whereas, at the X-axis we can visualize the features derived. Further annotation from the figure can be given as,

Table 4-2 P-value Plot Annotation

Plot Line	**Metadata**
Off white bar	Normal vs. Phone Scenario
Inverted delta marker with yellow color	Normal vs. Question Scenario
Blue diamond marker	Normal vs. Text Scenario
Black dash line at Y=0.05	Threshold reference line for best feature selection

Table 4-3 P-Value Analysis [2-Second Window]

P-Value Analysis [Normal Vs. Phone]

Features	**S1**	**S2**	**S3**	**S4**	**S5**	**S6**	**S7**	**S8**	**Actual Counts**	**Cumulative Counts**
AvgHR	0.0870	0.2492	0.0132	0.4441	0.0368	0.7425	0.2103	0.9874	3.00	3.00
Average_HRV	0.0751	0.0008	0.4902	0.7546	0.0099	0.1080	0.5021	0.9944	3.00	3.00
NN50	0.9997	0.9942	0.7330	0.2916	1.0000	0.3411	0.5000	0.0000	1.00	1.00
pNN50	0.8598	0.9358	0.7330	0.5375	0.9992	0.0489	0.2221	0.0056	2.00	2.00

SE	0.1077	0.0000	0.0228	0.0000	0.0000	0.5440	0.2799	0.9985	4.00	2.00
PSE	0.0001	0.0000	0.9986	0.9958	0.0000	0.0746	0.2045	0.9974	4.00	4.00
SD_HR	0.0003	0.0000	1.0000	0.3975	0.0000	0.0015	0.2476	0.2014	4.00	4.00
SD_RR	0.0365	0.8758	0.0004	0.0608	1.0000	1.0000	0.8259	0.9802	3.00	3.00
RMSSD	0.1478	0.0297	0.1154	0.6054	0.0535	0.1455	0.5164	0.9937	2.00	2.00
MeanRR	0.0751	0.0008	0.4902	0.7546	0.0099	0.1080	0.5021	0.9944	3.00	3.00

P-Value Analysis [Normal Vs. Question]

Features	**S1**	**S2**	**S3**	**S4**	**S5**	**S6**	**S7**	**S8**	**Actual Counts**	**Cumulative Counts**
AvgHR	0.6391	0.9950	0.0025	0.2494	0.9984	0.7879	0.0890	0.9795	2.00	5.00
Average_HRV	0.0144	0.5534	0.0004	0.1041	0.7021	0.8546	0.0488	0.2466	3.00	6.00
NN50	0.9998	0.5000	1.0000	0.9634	0.2370	0.0000	0.9993	0.0130	2.00	3.00
pNN50	0.9981	0.9490	0.9994	0.9799	0.4016	0.0005	0.7644	0.0055	2.00	4.00
SE	0.0000	0.0000	0.0000	0.0000	0.0000	1.0000	0.0258	1.0000	6.00	10.00
PSE	0.0683	0.9838	0.0000	0.9603	0.0043	1.0000	0.0049	0.0001	5.00	9.00
SD_HR	0.0004	0.0000	0.9852	0.5451	0.0001	0.5479	0.4580	0.0000	4.00	8.00
SD_RR	0.0222	1.0000	0.0000	0.0636	0.9732	1.0000	0.4279	0.9999	3.00	6.00
RMSSD	0.0142	0.7261	0.0025	0.0124	0.7002	0.8353	0.0366	0.6614	4.00	6.00
MeanRR	0.0144	0.5534	0.0004	0.1041	0.7021	0.8546	0.0488	0.2466	3.00	6.00

P-Value Analysis [Normal Vs. Text]

Features	**S1**	**S2**	**S3**	**S4**	**S5**	**S6**	**S7**	**S8**	**Actual Counts**	**Cumulative Counts**
AvgHR	0.0811	0.0024	0.0000	0.0017	0.0031	0.0007	0.1816	0.8924	6.00	11.00
Average_HRV	0.0013	0.0000	0.0001	0.0000	0.0019	0.0000	0.0278	0.8315	7.00	13.00
NN50	0.9666	1.0000	1.0000	1.0000	1.0000	1.0000	0.3476	0.0099	1.00	4.00
pNN50	0.3699	0.9999	0.9280	0.9951	0.9532	0.9987	0.2130	0.0732	1.00	5.00
SE	0.0000	0.0000	0.0000	0.0000	0.0000	0.0000	1.0000	1.0000	6.00	16.00
PSE	0.0000	0.0000	0.0000	0.0000	0.0000	0.0000	0.7028	0.6025	6.00	15.00
SD_HR	0.2004	0.0055	0.8262	0.0032	0.0000	0.0000	0.5113	0.9300	4.00	12.00
SD_RR	0.0200	1.0000	1.0000	0.9625	1.0000	1.0000	0.1738	0.0000	2.00	8.00
RMSSD	0.0030	0.0000	0.0001	0.0000	0.0046	0.0000	0.0387	0.8544	7.00	13.00
MeanRR	0.0013	0.0000	0.0001	0.0000	0.0019	0.0000	0.0278	0.8315	7.00	13.00

(note: values are rounded to 4 decimal places)

Table 4-4 P-Value Analysis [2-Second Window]

P-Value Analysis [Normal Vs. Phone]

Features	S1	S2	S3	S4	S5	S6	S7	S8	Actual Counts	Cumulative Counts
AvgHR	0.0000	0.9809	0.0000	0.8962	0.0000	0.0000	0.0000	0.0636	6.00	6.00
Average_HRV	0.0000	0.9317	0.0000	0.0366	0.0000	0.0000	0.0000	0.1095	6.00	6.00
NN50	0.0906	0.0000	0.0000	0.0000	0.0000	0.0007	0.0728	0.0549	8.00	8.00
pNN50	0.0000	0.0257	0.0038	0.0014	0.9988	0.0001	0.0345	0.0274	7.00	7.00
SE	0.0000	0.0000	0.0000	0.0000	0.0000	0.0000	0.0000	0.0001	8.00	8.00
PSE	0.4543	0.0000	0.0079	0.0000	0.0003	0.6078	0.0677	0.3103	5.00	5.00
SD_HR	0.0000	0.0000	0.0048	0.5665	0.0014	0.0000	0.0000	0.3050	6.00	6.00
SD_RR	0.9954	0.0000	0.0000	0.2527	0.0000	0.0000	0.0000	0.2395	5.00	5.00
RMSSD	0.0000	0.7213	0.0000	0.0188	0.0000	0.0000	0.0000	0.1867	6.00	6.00
MeanRR	0.0000	0.9317	0.0000	0.0366	0.0000	0.0000	0.0000	0.1095	6.00	6.00

P-Value Analysis [Normal Vs. Question]

Features	S1	S2	S3	S4	S5	S6	S7	S8	Actual Counts	Cumulative Counts
AvgHR	0.0177	0.0000	0.0000	0.0396	0.0000	0.0000	0.3975	0.4043	6.00	12.00
Average_HRV	0.0024	0.0000	0.0000	0.0000	0.1785	0.0000	0.1034	0.5630	5.00	11.00
NN50	0.5232	0.0000	0.0000	0.0000	0.0000	0.0000	0.1009	0.1520	5.00	13.00
pNN50	0.0000	0.0000	0.0002	0.0000	0.0999	0.0000	0.1149	0.2771	6.00	13.00
SE	0.0008	0.0012	0.0000	0.0000	0.0000	0.0000	0.0000	0.0000	8.00	16.00
PSE	0.0003	0.0016	0.0000	0.0000	0.8928	0.0000	0.2409	0.0103	6.00	11.00
SD_HR	0.0000	0.0000	0.0000	0.0000	0.0000	0.0000	0.0000	0.0199	8.00	14.00
SD_RR	0.5747	0.0000	0.0000	0.0000	0.0000	0.0051	0.0000	0.0044	7.00	12.00
RMSSD	0.0052	0.0000	0.0000	0.0000	0.2453	0.0000	0.0873	0.8233	7.00	13.00
MeanRR	0.0024	0.0000	0.0000	0.0000	0.1785	0.0000	0.1034	0.5630	5.00	11.00

P-Value Analysis [Normal Vs. Text]

Features	S1	S2	S3	S4	S5	S6	S7	S8	Actual Counts	Cumulative Counts
AvgHR	0.0004	0.0000	0.0000	0.0000	0.0000	0.0000	0.1197	0.1628	6.00	17.00
Average_HRV	0.0015	0.0000	0.0000	0.0000	0.0000	0.0000	0.3511	0.2920	6.00	18.00
NN50	0.0000	0.0000	0.0000	0.0000	0.0000	0.0000	0.0013	0.0005	8.00	21.00

pNN50	0.0001	0.0000	0.9204	0.0000	0.0000	0.9804	0.0150	0.0025	8.00	21.00
SE	0.0000	0.0000	0.0000	0.0000	0.0000	0.0000	0.0000	0.0000	8.00	24.00
PSE	0.0033	0.0622	0.0000	0.0001	0.0000	0.0000	0.0233	0.9960	7.00	18.00
SD_HR	0.0000	0.0000	0.0000	0.0084	0.0000	0.0000	0.3540	0.4574	6.00	20.00
SD_RR	0.0243	0.0000	0.5089	0.0049	0.0000	0.0728	0.0107	0.7536	6.00	18.00
RMSSD	0.0604	0.0000	0.0000	0.0000	0.0000	0.0000	0.3439	0.3379	6.00	19.00
MeanRR	0.0015	0.0000	0.0000	0.0000	0.0000	0.0000	0.3511	0.2920	6.00	17.00

(note: values are rounded to 4 decimal places)

Observing the given plot in figure 4.13 we can come to the conclusion that better statistical significance is observed in case of normal vs. text scenario since the maximum amount of distraction is concentrated in this phase.

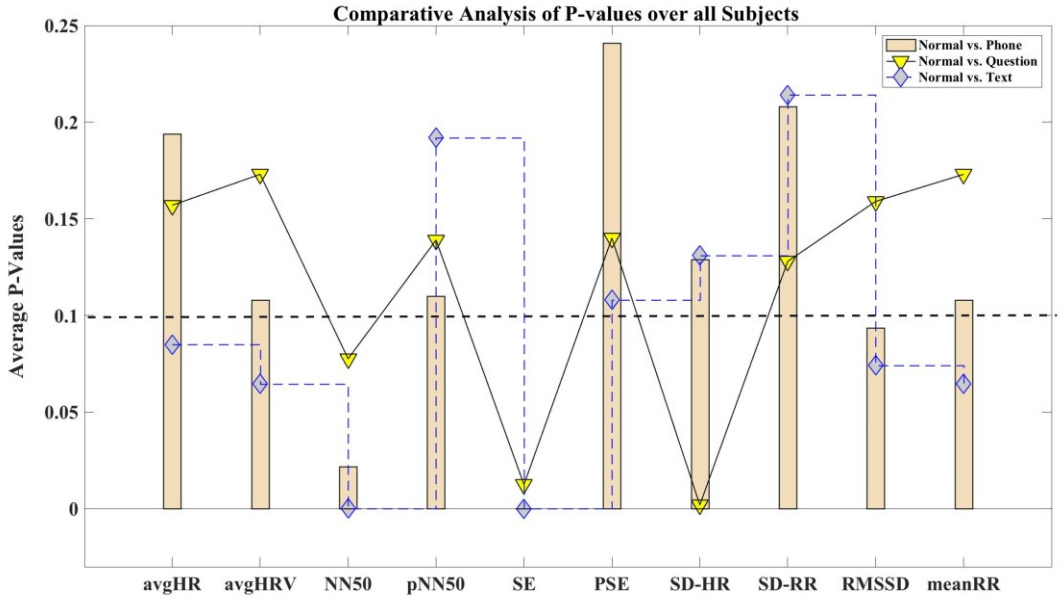

Figure 4:12 comparative Analysis of P-values over all Features over all Subjects

4.1.3 Multivariate Analysis and Identification Results

This section makes use of various extracted features as dimensions of multi-variate space containing useful insights; ranging from pre-distraction to post-distraction scenarios. We used

MATLAB classification learner to train and test the predictive models. The main advantage of using MATLAB toolbox is its extensive inclusion of multiple libraries of machine learning algorithms that can be trained and tested over one data. This allows multiple insights from different classifiers to validate and choose the best that suits the predictive need of the data. Table 4.5 shows the distraction identification accuracies of the windows of ECG data with different labels named normal, phone, question and text. Classification accuracies reported in the above table are the notion of correctly classified instances which can be expressed as follows,

$$Classification\ Accuracy = \frac{\sum True\ Positive + \sum True\ Negatives}{Total\ Population} \quad (2.19)$$

Table 4-5 Classifier Identification Accuracies

2 Second Segmentation Results

Algorithm and Subjects	Decision Tree	SVM-Poly2D	SVM -Poly3D	1-NN
S1	94.38%	95.97%	97.77%	95.31%
S2	87.44%	86.36%	88.43%	83.10%
S3	91.13%	91.29%	93.45%	91.45%
S4	92.81%	78.18%	86.76%	85.45%
S5	86.81%	84.13%	85.03%	81.38%
S6	91.06%	85.84%	87.17%	91.94%
S7	88.46%	89.10%	90.38%	83.12%
S8	71.98%	81.64%	77.29%	71.57%
Average Accuracy	88.01%	86.56%	88.29%	85.42%

4 Second Segmentation Results

Algorithm and Subjects	Decision Tree	SVM-Poly2D	SVM -Poly3D	1-NN
S1	93.12%	93.98%	91.83%	90.09%

S2	88.75%	93.72%	92.50%	88.82%
S3	95.96%	95.15%	94.99%	95.42%
S4	94.11%	93.49%	92.97%	92.40%
S5	90.86%	95.84%	95.84%	95.54%
S6	87.79%	80.07%	75.94%	79.32%
S7	87.32%	88.73%	84.51%	87.32%
S8	76.04%	79.17%	79.17%	71.88%
Average Accuracy	89.24%	90.02%	88.47%	87.60%

Where true positives are the correctly labeled instances of positive class and true negatives are the instances belonging to the negative class labeled correctly as negative instances. From above classification table we can confirm that SVM-Poly2D, and SVM-Poly3D performed consistently over all subjects. At subject 3 over 4 second window we observed maximum prediction accuracy of 95.93% which is the highest classification accuracy observed over all subjects. It can also be inferred from above results that 4 second windowing performed better in classification by providing more resolution and depth in time as compared to the 2 second windowing approach.

4.2 Results (Wavelet as a Filter Bank Approach)

In this effort, all preprocessing, segmentation, wavelet packet decomposition, feature extraction, and predictive modeling is performed in MATLAB software.

4.2.1 Wavelet Packet Based SubBand Selection

We applied multi-signal wavelet packet transform as explained in 3.1, after which based on optimal statistical significant difference, we shortlist wavelet packets in terms of normal vs distracted scenarios (either normal vs. phone or normal vs. question). We set the threshold of t=3 by converting the p-value space into logarithmic transformation to normalize the sequences. The p-values greater than t=3 will have higher statistical significance with significantly lower value

of p<0.001. Following figure shows the sample P scores for the wavelet packet transformation level 7 subBands ranging from 0 to 30 Hz for subject 1.

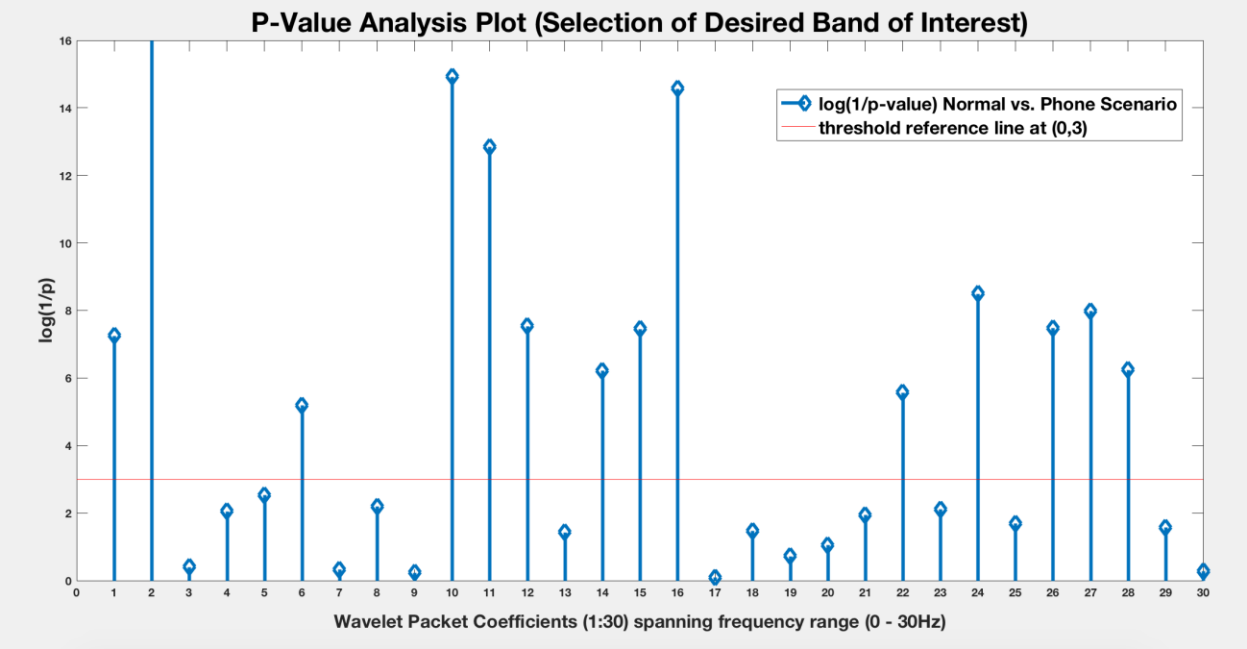

Figure 4:13 subBand Selection p-value Analysis Plot

In order to access the predictive capability of the system, we performed classification learning based on aforementioned 4 feature spaces. Following table explains the predictive model capabilities. Features predictive model assessment states that the predictive capability of the system is enhanced by employing feature selection using subBandSelect approach by selecting more relevant features for the detection task. The number of dimensions in the baseline is 384 (128 levels x 3 leads). The WPT subBand selection reduced the dimensionality close to ~20 features on an average, which takes it to ~60 features considering 3 features per selected subBand. As reported in the following tables, the prediction performance of the subBandSelect features is 50.04% compared to the performance of baseline features, which is 44.10% using 1-NN classifier (i.e. K=1).

Other than 1-NN, we employed model-based prediction approach using decision tree, in order to access an impact of discriminative transformation on WPT features in machine learning. Here to tune the decision tree we used GINI index with depth limit of 20. Table 4.6 reports the results from 4 different identification cases using decision tree classifier. Demonstrated that the decision tree is capable of generating the higher accuracy baseline by selecting 20 best in class features, thereby reduces the redundancy in model training.

Table 4-6 Distraction Identification Results using Decision Tree

Subject	**Decision Tree**			
	Baseline	**subBandSelect**	**subBandSelect + LDA**	**subBandSelect + K-LDA**
1	62.17	63.27	73.23	96.02
2	68.43	67.28	67.99	90.48
3	91.85	91.61	93.84	91.01
4	60.99	64.59	67.02	74.84
5	61.79	60.37	62.93	81.25
6	68.44	68.81	64.04	92.66
7	69.86	78.77	85.27	86.64
8	88.97	88.28	89.31	100
Average	**71.56**	**72.87**	**75.45**	**89.11**

Table 4-7 Distraction Identification Results using 1-NN

Subject	**1-NN**			
	Baseline	**SubBandSelect**	**SubBandSelect + LDA**	**SubBandSelect+ K-LDA**
1	42.04	48.01	69.47	95.35
2	42.33	48.24	64.99	91.36

3	39.43	53.74	94.34	90.85
4	41.86	44.82	66.17	73.57
5	44.74	48.44	63.21	78.84
6	46.24	48.81	69.91	91.01
7	46.52	54.11	84.93	86.64
8	49.66	54.14	90.34	100
Average	**44.10**	**50.03**	**75.42**	**88.45**

4.2.2 Linear Discriminant Dimensionality Reduction

Wavelet Packet Decomposition approach yields the improved prediction accuracy of the model. However, this improved prediction accuracy is not sufficient enough to generate reliability across the prediction. Taking into consideration of subBandSelect features (i.e. ~60), we hypothesize that the issue raised because of the curse of dimensionality. Therefore, employing LDA in subBandSelect feature space makes sense to discriminatively transform the given feature space into reduced feature space.

As illustrated in the table 4.6 the prediction accuracy got improved after implementation of discriminative transformation on the existing space. There is a shift of 25% increase in prediction accuracy observed between the regular subBandSelect feature space with ~50% prediction accuracy on an average to discriminative LDA transformed space having ~75% prediction accuracy. This shows that the LDA successfully removes the curse of dimensionality, with the retention of discriminative capability of the predictive model. Following figure illustrates the scatter plot of LDA generated feature space.

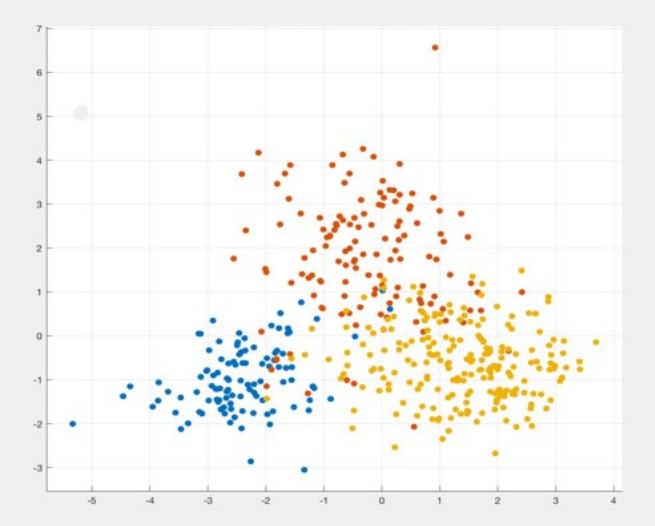

Figure 4:14 subBandSelect + LDA Feature Space Scatter Plot

Here in the above figure, the color scheme represents the following

Table 4-8 Color Scheme for LDA Transformed Space

Color	**Class**
Blue	Normal Driving
Red	Phone Conversation (Cognitive Distracted Driving)
Yellow	Conversation with Passenger (Cognitive + Visual Distracted Driving)

3.7.3 Non-Linear Discriminative Dimensionality Reduction Using Kernels

After successful implementation of the LDA transformed space, we felt the need to make the predictive model more robust and non-linear. Therefore, we employed Gaussian Kernel; after several iterative steps we select the variance=1, which renders optimized class separation. Here in table 4.15 we can analyze this class separation in terms of correctly classified instance rate

(accuracy) increase, this is induced by achieving optimum non-linear feature space transformation through non-linear subspaces. This posed an increase in the classification accuracy from ~75% to ~88% using K-LDA. Following figure shows the dramatic reduction in the discrimination between classes in the new space using non-linear mapping.

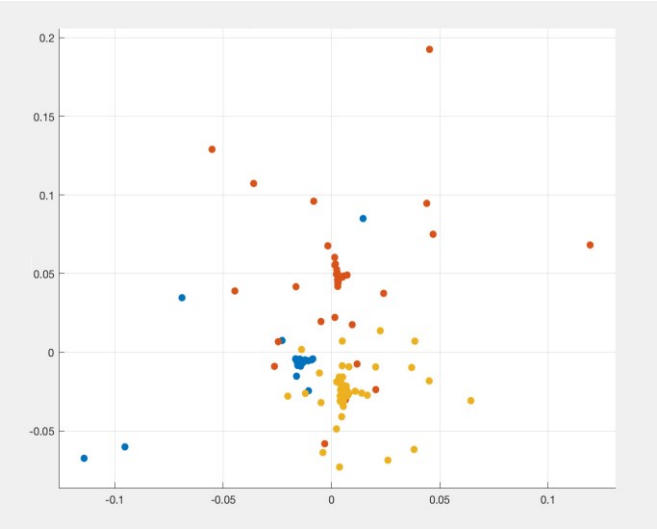

Figure 4:15 subBandSelect + K-LDA Feature Space Scatterplot

Here in the above figure color scheme represents the following,

Table 4-9 Color Scheme for K-LDA Transformed Space

Color	**Class**
Blue	Normal Driving
Red	Phone Conversation(Cognitive Distracted Driving)
Yellow	Conversation with Passenger(Cognitive + Visual Distracted Driving)

Chapter 5 Conclusion

The primary intention of this study is to investigate the impact of secondary workload on driver's cognitive state of mind. We employed two short window real-time analytic processing approach on well-established ECG features, we did complex yet effective evaluation and validation of the extracted ECG features, thus inferred the concrete reference of causality relationship between physiological state and drivers cognitive state of mind. In addition, to this we studied multi-variate feature orientation with respect to access the classification capability of the overall predictive model. The predictive accuracies show ~98% prediction of distraction in real-time. Feature Engineering followed by wavelet as a filter bank approach also gave significant results.

The important intent behind usage of Wavelet Packet Decomposition was to identify the frequency subBands with higher variance in feature sub-space, triggered by different distraction scenarios compared with normal driving. We came up with subBandSelect approach powered by higher deflection in p-values between normal and distracted scenarios from set of statistical features derived from each case scenario. Further which we introduced discriminative analysis approach to bring the feature space into maximum separation between classes to enhance predictive capability of the model. The newly generated discriminative space yields an increase in classification accuracy by retaining the discrimination in reduced space with elimination of curse of dimensionality. In order to free the linear correlation in the LDA transformation we then apply kernel non-linear discriminative analysis, which lead to higher between-class separation with lower in class variance, thus thereby maximizing distraction detection capability.

Bibliography

Vegega, M., Jones, B., & Monk, C. (2013). Understanding the effects of distracted driving and developing strategies to reduce resulting deaths and injuries: a report to Congress(No. DOT HS 812 053). United States. Office of Impaired Driving and Occupant Protection.

National Highway Traffic Safety Administration. Facts and Statis- tics. [Online]. Available: https://www.nhtsa.gov/risky-driving/distracted- driving. [Accessed: 30-Jul-2017].

National Highway Traffic Safety Administration. (2013). Traffic safety facts 2011 data--pedestrians. Annals of emergency medicine, 62(6), 612.

Nakayama, O., Futami, T., Nakamura, T., & Boer, E. R. (1999). Development of a steering entropy method for evaluating driver workload (No. 1999-01-0892). SAE Technical Paper.

Rongben, W., Lie, G., Bingliang, T., & Lisheng, J. (2004, October). Monitoring mouth movement for driver fatigue or distraction with one camera. In Intelligent Transportation Systems, 2004. Proceedings. The 7th International IEEE Conference on (pp. 314-319). IEEE.

You, C. W., Lane, N. D., Chen, F., Wang, R., Chen, Z., Bao, T. J., ... & Campbell, A. T. (2013, June). Carsafe app: Alerting drowsy and distracted drivers using dual cameras on smartphones. In Proceeding of the 11th annual international conference on Mobile systems, applications, and services(pp. 13-26). ACM.

Fernández, A., Usamentiaga, R., Carús, J. L., & Casado, R. (2016). Driver distraction using visual-based sensors and algorithms. Sensors, 16(11), 1805.

Alizadeh, V., & Dehzangi, O. (2016, November). The impact of secondary tasks on drivers during naturalistic driving: Analysis of EEG dynamics. In Intelligent Transportation Systems (ITSC), 2016 IEEE 19th International Conference on (pp. 2493-2499). IEEE.

Peng, R. C., Zhou, X. L., Lin, W. H., & Zhang, Y. T. (2015). Extraction of heart rate variability from smartphone photoplethysmograms. Computational and mathematical methods in medicine, 2015.

Cohen, Z., & Haxha, S. (2017). Optical-based sensor prototype for continuous monitoring of the blood pressure. IEEE Sensors Journal, 17(13), 4258-4268.

Z. Zhang, Z. Pi, S. Member, and B. Liu, TROIKA: A General Frame- work for Heart Rate Monitoring Using Wrist-Type Photoplethysmo- graphic (PPG) Signals During Intensive Physical Exercise, vol. 9294, no. c, pp. 110, 2014

Taherisadr, Mojtaba, Omid Dehzangi, and Hossein Parsaei. ”Single Channel EEG Artifact Identification Using Two-Dimensional Multi- Resolution Analysis.” Sensors 17.12 (2017): 2895.

Dehzangi, Omid, Mojtaba Taherisadr, and Raghvendar ChangalVala. ”IMU-Based Gait Recognition Using Convolutional Neural Networks and Multi-Sensor Fusion.” Sensors 17.12 (2017): 2735.

Z.Zhang,Photoplethysmography-basedheartratemonitoringinphysical activities via joint sparse spectrum reconstruction, IEEE Trans. Biomed. Eng., vol. 62, no. 8, pp. 19021910, 2015.

M. S. Islam, M. Shifat-E-Rabbi, A. M. A. Dobaie, and M. K. Hasan, PREHEAT: Precision heart rate monitoring from intense motion artifact corrupted PPG signals using constrained RLS and wavelets, Biomed. Signal Process. Control, vol. 38, pp. 212223, 2017.

A. Galli, G. Frigo, C. Narduzzi, and G. Giorgi, Robust Estimation and Tracking of Heart Rate by PPG Signal Analysis, pp. 05, 2017.

D. Jarchi, A. J. Casson, and S. Member, Estimation of heart rate from foot worn photoplethysmography sensors during fast bike exercise, 2016 38th Annu. Int. Conf. IEEE Eng. Med. Biol. Soc., pp. 21583155, 2016.

D. Jarchi, A. J. Casson, and S. Member, Photoplethysmogram and Electrocardiogram based estimation of instantaneous heart rate during physical activity, vol. 9294, no. c, 2017.

Skinner, James E., Jerry M. Anchin, and Daniel N. Weiss. ”Nonlinear analysis of the heartbeats in public patient ECGs using an automated PD2i algorithm for risk stratification of arrhythmic death.” Therapeutics and clinical risk management 4.2 (2008): 549.

Skinner, James E., et al. ”Comparison of linearstochastic and nonlin- eardeterministic algorithms in the analysis of 15-minute clinical ECGs to predict risk of arrhythmic death.” Therapeutics and clinical risk management 5 (2009): 671.

Volz, H-P., et al. ”Afferent connections of the nucleus centralis amyg- dalae.” Anatomy and embryology 181.2 (1990): 177-194.

Henderson, Luke A., et al. ”Functional magnetic resonance signal changes in neural structures to baroreceptor reflex activation.” Journal of Applied Physiology 96.2 (2004): 693-703.

Kemp, Andrew H., et al. ”Impact of depression and antidepressant treatment on heart rate variability: a review and meta-analysis.” Biological psychiatry 67.11 (2010): 1067-1074.

Kher, Rahul, et al. ”Implementation of derivative based QRS complex detection methods.” Biomedical Engineering and Informatics (BMEI), 2010 3rd International Conference on. Vol. 3. IEEE, 2010.

Arteaga-Falconi,Juan,HusseinAlOsman,andAbdulmotalebElSaddik. ”R-peak detection algorithm based on differentiation.” Intelligent Signal Processing (WISP), 2015 IEEE 9th International Symposium on. IEEE, 2015.

L. Yu, X. Sun, and K. Zhang, Driving distraction analysis by ECG signals: An entropy analysis, Lect. Notes Comput. Sci. (including Subser. Lect. Notes Artif. Intell. Lect. Notes Bioinformatics), vol. 6775 LNCS, pp. 258264, 2011.

M.Mahachandra,Yassierli,I.Z.Sutalaksana,andK.Suryadi,Sensitivity of heart rate variability as indicator of driver sleepiness, 2012 Southeast Asian Netw. Ergon. Soc. Conf. Ergon. Innov. Leveraging User Exp. Sustain. SEANES 2012, pp. 05, 2012.

I. Bichindaritz, C. Breen, E. Cole, N. Keshan, and P. Parimi, Feature Selection and Machine Learning Based Multilevel Stress Detection from ECG Signals, Springer, Cham, 2018, pp. 202213.

K. Ito, S. Usuda, K. Yasunaga, and M. Ohkura, Evaluation of Feelings of Excitement Caused by a VR Interactive System with Unknown Experience Using ECG, Springer, Cham, 2018, pp. 292302.

S. V. Deshmukh and O. Dehzangi, ECG-Based Driver Distraction Iden- tification Using Wavelet Packet Transform and Discriminative Kernel- Based Features, in 2017 IEEE International Conference on Smart Com- puting (SMARTCOMP), 2017, pp. 17.

S. Deshmukh and O. Dehzangi, Identification of real-time driver dis- traction using optimal subBand detection powered by Wavelet Packet Transform, in 2017 IEEE 14th International Conference on Wearable and Implantable Body Sensor Networks (BSN), 2017, pp.

O. Dehzangi and C. Williams, Towards multi-modal wearable driver monitoring: Impact of road condition on driver distraction, 2015 IEEE 12th Int. Conf. Wearable Implant. Body Sens. Networks, BSN 2015, pp. 16, 2015.

V. Alizadeh and O. Dehzangi, The impact of secondary tasks on drivers during naturalistic driving: Analysis of EEG dynamics, IEEE Conf. Intell. Transp. Syst. Proceedings, ITSC, pp. 24932499, 2016.

O. Dehzangi and C. Williams, Towards multi-modal wearable driver monitoring: Impact of road condition on driver distraction, 2015 IEEE 12th Int. Conf. Wearable Implant. Body Sens. Networks, BSN 2015, pp. 16, 2015.

V. Alizadeh and O. Dehzangi, The impact of secondary tasks on drivers during naturalistic driving: Analysis of EEG dynamics, IEEE Conf. Intell. Transp. Syst. Proceedings, ITSC, pp. 24932499, 2016.

A.Burnsetal.,SHIMMER???:Anextensibleplatformforphysiological signal capture, 2010

Annu. Int. Conf. IEEE Eng. Med. Biol. Soc. EMBC10, pp. 37593762, 2010.

S. Chernenko, ECG processing R-peaks detection Librow Software. [Online]. Available: http://www.librow.com/cases/case-2. [Accessed: 18- Jun-2017].

Y. Freund and L. Mason, The alternating decision tree learning algo- rithm, Proceeding Sixt. Int. Conf. Mach. Learn., p. 10 str., 1999.

J. M. Keller and M. R. Gray, A Fuzzy K-Nearest Neighbor Algorithm, IEEE Trans. Syst. Man Cybern., vol. SMC-15, no. 4, pp. 580585, 1985.

C. Cortes, C. Cortes, V. Vapnik, and V. Vapnik, Support Vector Net- works, Mach. Learn., vol. 20, no. 3, p. 273 - 297, 1995.

F.P.daSilva,MentalWorkload,TaskDemandandDrivingPerformance: What Relation?, Procedia - Soc. Behav. Sci., vol. 162, pp. 310319, Dec. 2014

P. A. Hancock and P. A. Desmond, Stress, workload, and fatigue. 2001. [41] A. L. Hansen, B. H. Johnsen, and J. F. Thayer, Vagal influence on working memory and attention, Int. J. Psychophysiol., vol. 48, no. 3, pp.263274, 2003.

N. a. C. Cressie and H. J. Whitford, How to Use the Two Samplet-Test, Biometrical J., vol. 28, no. 2, pp. 131148, 1986.

D. G. Stork and E. Yom-Tov, Computer Manual in MATLAB to accompany Pattern Classification, p. 136, 2004.

R.P.W. Duin, P. Juszczak, D. de Ridder, P. Paclik, E. Pekalska, and D.M.J. Tax,PRTools, a Matlab toolbox for pattern recognition, http://www.prtools.org, 2004.

Meinicke, Peter, et al. ”Improving transfer rates in brain computer interfacing: a case study.” Advances in Neural Information Processing Systems. 2003.

Liang, Yulan, Michelle L. Reyes, and John D. Lee. "Real-time detection of driver cognitive distraction using support vector machines." IEEE transactions on intelligent transportation systems 8.2 (2007): 340-350.

Gallahan, Sean L., et al. "Detecting and mitigating driver distraction with motion capture technology: Distracted driving warning system." Systems and Information Engineering Design Symposium (SIEDS), 2013 IEEE. IEEE, 2013.

Lin, Chin-Teng, et al. "Spatial and temporal EEG dynamics of dual-task driving performance." Journal of NeuroEngineering and rehabilitation 8.1 (2011): 11.

Kim, Jin Yong, et al. "Highly reliable driving workload analysis using driver electroencephalogram (EEG) activities during driving." International Journal of Automotive

Technology 14.6 (2013): 965-970.

R. N. Khushaba, S. Kodagoa, S. Lal, and G. Dissanayake, “Driver Drowsiness Classification Using Fuzzy Wavelet Packet Based Feature Extraction Algorithm”, IEEE Transaction on Biomedical Engineering, vol. 58, no. 1, pp. 121-131, 2011.

R. R. Coifman, Y. Meyer, S. Quake, and V. Wickerhauser, ”Wavelet analysis and Signal processing”, In: Wavelets and Their Applications. Jones and Barlett, pp. 153-178, 1992.

K. Englehart,”Signal representation for classification of the transient myoelectric signal”, PhD Thesis, Department of Electrical and Computer Engineering, University of New Brunswick, Fredericton, NB, Canada, 1998.

S. Mallat, “A wavelet tour of signal processing: The sparse way”, third edition, Academic Press, 2009.

R. N. Khushaba, A. Al-Jumaily, and A. Al-Ani, “Novel Feature Extraction Method based on Fuzzy Entropy and Wavelet Packet Transform for Myoelectric Control”, 7th International Symposium on Communications and Information Technologies ISCIT2007, Sydney, Aus

Burns, Adrian, et al. "SHIMMERTM: an extensible platform for physiological signal capture." Engineering in Medicine and Biology Society (EMBC), 2010 Annual International Conference of the IEEE. IEEE, 2010.

Vasilescu, M. Alex O., and Demetri Terzopoulos. "Multilinear analysis of image ensembles: Tensorfaces." European Conference on Computer Vision. Springer Berlin Heidelberg, 2002.

Liu, Chengjun, and Harry Wechsler. "A shape-and texture-based enhanced Fisher classifier for face recognition." IEEE transactions on image processing 10.4 (2001): 598-608.

Schölkopf, Bernhard, Alexander Smola, and Klaus-Robert Müller. "Nonlinear component analysis as a kernel eigenvalue problem." Neural computation 10.5 (1998): 1299-1319.

Ye, Fei, Zhiping Shi, and Zhongzhi Shi. "A comparative study of PCA, LDA and Kernel LDA for image classification." Ubiquitous Virtual Reality, 2009. ISUVR'09. International Symposium on. IEEE, 2009.

Pavlidis, I., et al. "Dissecting Driver Behaviors Under Cognitive, Emotional, Sensorimotor, and Mixed Stressors." Scientific reports 6 (2016).

Safavian, S. Rasoul, and David Landgrebe. "A survey of decision tree classifier methodology." IEEE transactions on systems, man, and cybernetics 21.3 (1991): 660-674.

Larose, Daniel T. "k-Nearest Neighbor Algorithm." Discovering Knowledge in Data: An Introduction to Data Mining (2005): 90-106.

John Lu, Z. Q. "The elements of statistical learning: data mining, inference, and prediction." Journal of the Royal Statistical Society: Series A (Statistics in Society) 173.3 (2010): 693-694.

Fig. 1 Shimmer ECG Sensor and Electrode Plcaement Setup. Example positioning of the electrodes for ECG measurement with 9” leads. Shimmer ECG documentation available at webiste address . <http://www.shimmersensing.com/images/uploads/docs/ECG_User_Guide_

ECG image source: https://www.cablesandsensors.com/pages/12-lead-ecg-placement-guide-with-illustrations